

Joint empirical risk minimization for instance-dependent positive-unlabeled data

Wojciech Rejchel^a, Paweł Teisseyre^{b,c,*}, Jan Mielniczuk^{b,c},

^aNicolaus Copernicus University, Toruń, Poland

^bPolish Academy of Sciences, Warsaw, Poland

^cWarsaw University of Technology, Warsaw, Poland

Abstract

Learning from positive and unlabeled data (PU learning) is actively researched machine learning task. The goal is to train a binary classification model based on a training dataset containing part of positives which are labeled, and unlabeled instances. Unlabeled set includes remaining part of positives and all negative observations. An important element in PU learning is modeling of the labeling mechanism, i.e. labels' assignment to positive observations. Unlike in many prior works, we consider a realistic setting for which probability of label assignment, i.e. propensity score, is instance-dependent. In our approach we investigate minimizer of an empirical counterpart of a joint risk which depends on both posterior probability of inclusion in a positive class as well as on a propensity score. The non-convex empirical risk is alternately optimised with respect to parameters of both functions. In the theoretical analysis we establish risk consistency of the minimisers using recently derived methods from the theory of empirical processes. Besides, the important development here is a proposed novel implementation of an optimisation algorithm, for which sequential approximation of a set of positive observations among unlabeled ones is crucial. This relies on modified technique of 'spies' as well as on a thresholding rule based on conditional probabilities. Experiments conducted on 20 data sets for various labeling scenarios show that the proposed method works on par or more effectively than state-of-the-art methods based on propensity function estimation.

Keywords: positive-unlabeled learning, propensity score estimation, empirical risk minimization, selected at random assumption, risk consistency

1. Introduction

1.1. PU learning

Positive-unlabeled (PU) learning is a machine learning task that aims to fit a binary classification model based on data with partially assigned labels [1]. In this scenario, some instances from a positive class retain true labels, while for the remaining instances, no labels have been assigned (they can belong either to positive or negative class). PU learning can be thus viewed as a variant of semi-supervised learning [2] when we have positive, negative and

*Corresponding author: Paweł Teisseyre (teisseyrep@ipipan.waw.pl)

unlabeled observations at our disposal; the difference is that in PU case we do not have observations with a negative label assigned. PU data appear in many practical applications. Consider reporting certain ailments, such as migraine attacks, using dedicated mobile applications [3]. Some patients report headaches on days when they occur. However, patients who do not report symptoms may include those who did not experience migraine, as well as those who experienced it but failed to report. Another example is detection of illegal content on social networks. Some profiles are reported as containing illegal content (positive cases). However, profiles not reported as illegal may also contain content that violates the law, but this has not been verified. PU data appear naturally in the classification of texts and images [4, 5, 6], anomaly detection [7], recommendation systems [8] and in many bioinformatics applications [9], where we often have a small set of positive observations (e.g. confirmed drug-drug interactions) and a large number of observations not assigned to any of the classes.

A key element of PU data analysis is modeling of the labeling mechanism that describes which of the positive observations are assigned a label. This is usually done by imposing some conditions on the probability of such action, called the propensity score function [1]. The simplest approach used for PU data is to assume that this probability is constant (Selected Completely at Random assumption, in short SCAR) [10], which significantly simplifies learning [11, 12, 13, 14, 15]. However, this assumption is often not met in practice. For example, probability that a patient who has had a migraine attack will report it, may depend on the level of pain but also on other less obvious factors, such as age or her/his handling of migraine reporting application. Similarly, patients who experience certain illness-related symptoms, are more likely to be diagnosed and test positive for the disease, whereas asymptomatic patients may remain largely undiagnosed. Much of recent research work, described below, has focused on a more realistic case when labeling is instance-dependent, in particular commonly adopting a less restrictive assumption, called Selected At Random (SAR), according to which the probability of labeling a positive observation depends solely on the observed feature vector [16, 17, 18, 19, 20, 21]. We also note that PU framework can be viewed as a special case of data with noisy labels, see [22, 23].

1.2. Related works

Presently study of PU learning refocuses from the scenario when labels are randomly assigned in a positive class independently from data (SCAR assumption) to the scenario when they may depend on attributes of these elements (SAR assumption). For an overview of PU learning under SCAR, we refer to [1]. Recently, some methods have been proposed for PU learning under SAR setting, mainly based on some modifications of loglikelihood methods tailored to the studied partial observability scenario. In particular, LBE method [24] uses Expectation-Maximisation (EM) algorithm and assumption (2) below. The Expectation step calculates conditional probabilities of class given labels and predictors, based on current estimates of parameters, whereas Maximisation step is based on the expectation of conditional likelihood of class indicators given data. SAR-EM [16] and TM [19] methods are based on alternate optimisation of empirical counterparts of separate Fisher consistent criteria for the posterior and the propensity score. The main difference between those two papers is the way in which criterion for propensity score is constructed.

Moreover, [19] introduced the concept of joint learning of posterior probability and propensity score which extends the method proposed in [14] for SCAR framework. The recent method [18] assumes that the propensity score is a linear function of the posterior probability for the true class variable, which is a special case of Probabilistic Gap (PG) Assumption [25]. Moreover, the method, called here PGLIN, uses the Positive Function data assumption, stating that for some part of the support of distribution of predictors posterior probability is equal to 1. Finally, in [20] and [21] deep learning approaches to Empirical Risk Minimisation Method under PU scenario are investigated. In contrast to previously discussed papers, parametric modelling of propensity score is avoided, but at the expense of assuming that probability of a positive class is given. From the theoretical perspective, we also refer to [26] where a bound on the expected excess risk is derived under assumption that the propensity function is known.

Finally, it is worth mentioning that there are two basic assumptions for PU data generation: single-sample scenario (SS) and case-control (CC) scenario [1]. The SS scenario, assumes that the training data set is an iid sample from a general population being a mixture of positive and negative cases, and the labeled observations are drawn from among the positive ones with a probability described by the propensity score function. In the CC scenario, the unlabeled data is drawn from a general population, and the labeled data is an iid sample from the positive class. In view of this, considering the SAR assumption and the propensity score estimation problem is natural in the case of the SS scenario. On the other hand, most of the work operating for CC, assumes SCAR [27, 28, 29, 30, 31, 32]. Considering the above discussion, the current work focuses on the SS scenario and SAR assumption and in the experiments we focus on the methods that directly estimate non-constant propensity scores.

1.3. Contribution and proposed method

The method proposed here is based on the observation that the posterior probability for the class label indicator (which indicates whether the observation is assigned a label or not) can be represented as the product of the posterior probability for the true class variable and the propensity score function. Taking advantage of this fact and assuming that the both functions can be modeled parametrically, we propose the optimization of the risk function for the class label indicator, with respect to parameters related to the propensity score function and the posterior probability for the true class variable. Due to the fact that both posterior and propensity are modelled as members of the same parametric family, the described approach suffers from lack of identifiability, i.e. the parameters of propensity score function and the probability for the true class variable can not be specified uniquely. However, if certain additional parametric assumptions are imposed on the posterior probability and the propensity score then both functions are identifiable up to their interchange. We consider a local minimiser of empirical risk and establish probabilistic bounds on its excess risk (Theorem 1) from which risk consistency of the minimiser defined in (6) below follows (Theorem 2). In practice, we need to effectively find this minimizer, which is not an obvious task due to identifiability issue and non-convexity of the empirical risk. To solve the problem, we propose an asymmetric procedure of risk minimisation which differs in the way both parameters are optimised. In each iteration, among the unlabeled observations, we select those that are most likely to be positive. Determining this set is a pivotal problem on which effectiveness of the whole procedure

relies and we propose a novel way to tackle this based on conditional probabilities and technique of spies [1, 33]. Subsequently, the determined set is used to estimate the propensity score function. Then, given the estimate of the propensity function, we optimize the joint risk function to find parameters for the true class variable (see flowchart in Figure 1). In the experiments, we refer to the proposed method as JERM (**J**oint **E**mpirical **R**isk **M**inimization).

Experiments conducted on 20 data sets, including tabular and image data, and 4 different labeling schemes, including the SCAR and SAR assumptions, show that JERM works comparably to or better than the previously considered methods described above.

Our contributions can be summarized as follows.

1. We analyze a joint empirical risk function including parameters for the posterior probability of the true class variable and the propensity score function.
2. We prove an upper bound on the excess risk for the local minimizer of the joint empirical risk function from which its risk consistency minimiser defined in (6) follows.
3. We propose a new algorithm JERM (**J**oint **E**mpirical **R**isk **M**inimization), based on the optimization of the joint risk function and the estimation of the propensity score using the spy technique.
4. We design and perform experiments that allow to compare of related methods for different labeling schemes and labeling frequencies.

2. Positive-unlabeled learning via joint risk optimization

2.1. Preliminaries

We consider a PU setting, where the triple (X, Y, S) is generated from some unknown distribution $P(X, Y, S)$, $X \in \mathbb{R}^p$ is feature vector, $Y \in \{0, 1\}$ is true class variable, which is not observed directly and $S \in \{0, 1\}$ is class label indicator. Value $S = 1$ indicates that the instance is labeled and thus positive, whereas $S = 0$ means that the instance is unlabeled. In PU learning it is assumed that $P(S = 1|X = x, Y = 0) = 0$, which means that negative examples cannot be labeled. We adopt single-sample scenario [1] in which it is assumed that iid random vectors (X_i, Y_i, S_i) for $i = 1, \dots, n$ are generated from $P(X, Y, S)$. Since Y_i is not observable, the PU training data is $\mathcal{D} = \{(X_i, S_i) : i = 1 \dots, n\}$. Observe that in the consider framework $s(x) = P(S = 1|X = x)$ can be estimated using PU training data \mathcal{D} . However, our goal is to estimate the posterior for the true class variable $y(x) = P(Y = 1|X = x)$. This task cannot be performed directly because we do not observe Y_i . We note that instance-dependent labeling can be naturally studied in a single-training sample scenario in contrast to case-control scenario in which two samples are available: one iid sample from positive class $P(X|Y = 1)$ and one from a general population $P(X)$.

It follows from the Law of Total Probability and assumption $P(S = 1|X = x, Y = 0) = 0$, that the posterior probabilities are related as

$$s(x) = e(x)y(x), \tag{1}$$

where the propensity score $e(x) = P(S = 1|Y = 1, X = x)$ is unknown and in a general case not constant. In view of (1), identification of posterior $y(x)$ and propensity score $e(x)$ is clearly impossible in general. However, if certain parametric assumptions are imposed on $y(x)$ and $e(x)$ then both functions are identifiable up to an interchange of $y(x)$ and $e(x)$ [19]. Let $\sigma(t) = 1/(1 + e^{-t})$ be a logistic function, a^T denotes transposed column vector a and $|a|_1 = \sum_{i=1}^p |a_i|$ for $a = (a_1, \dots, a_p)^T$. The following parametric assumption will be imposed.

Assumption 1. *Posterior probability $y(x)$ and the propensity score function $e(x)$ are described by logistic functions:*

$$y(x) = \sigma(\beta_*^T x), \quad e(x) = \sigma(\gamma_*^T x), \quad (2)$$

where β_* and γ_* are ground-truth unknown parameters and $|\beta_*|_1 > |\gamma_*|_1$.

If (2) is true, then $y(x)$ and $e(x)$ are identifiable up to their interchange [19, Theorem 1]. Additional condition $|\beta_*|_1 > |\gamma_*|_1$, ensures that the functions $y(x)$ and $e(x)$ are identifiable. The role of the l_1 norm played in these conditions is not essential and it may be replaced by any norm. The model (2) has been introduced in [24] and [19]; in the later reference it is called double logistic model. Obviously, **Assumption 1** corresponds to the SAR setting, because the propensity score function depends on the observed features. The assumption enables modeling a wide class of situations in which the probability of labeling depends on the feature vector through the sigmoid function. Importantly, we note that **Assumption 1** encompasses situations when $e(x)$ is not monotonically increasing function of $y(x)$ and thus Probabilistic Gap Assumption considered in [25, 18] is not met. The limitation of **Assumption 1** is the specific parametric form of the propensity score function.

Below, we introduce the joint risk function, which will be a core element of our method. For $a, b \in \mathbb{R}$ and $s \in \{0, 1\}$ a logistic loss function is

$$\phi(a, b, s) = -s \log[\sigma(a)\sigma(b)] - (1 - s) \log[1 - \sigma(a)\sigma(b)], \quad (3)$$

Let us denote a joint parameter by $\theta = (\beta, \gamma)$ and the ground-truth parameter by $\theta_* = (\beta_*, \gamma_*)$. The risk function is

$$Q(\theta) = \mathbb{E}\phi(\beta^T X, \gamma^T X, S), \quad (4)$$

where the expectation is taken with respect to both X and S . Moreover, its observable empirical counterpart (empirical risk) is

$$Q_n(\theta) = \frac{1}{n} \sum_{i=1}^n \phi(\beta^T X_i, \gamma^T X_i, S_i). \quad (5)$$

In the proposed approach, we minimize the above function with respect to β and γ in order to obtain estimators of these parameters.

Function (5) has been already considered in PU learning under SCAR assumption [34] and SAR assumption [19]. It has been shown in [19] that under Assumption 1, a vector $\theta_* = (\beta_*, \gamma_*)$ is the unique minimizer of $Q(\theta)$ over a set $\{\theta = (\beta, \gamma) : |\beta|_1 > |\gamma|_1\}$.

Table 1 contains the most important notations used in the paper.

Table 1: Summary of notation.

Notation	Meaning
n	number of instances
p	number of features
$X \in \mathbb{R}^p$	feature vector
$Y \in \{0, 1\}$	true class variable (not observed directly)
$S \in \{0, 1\}$	label indicator (observed directly)
$\mathcal{D} = \{(X_i, S_i) : i = 1 \dots, n\}$	PU training data
$y(x) = P(Y = 1 X = x)$	posterior probability of $Y = 1$
$s(x) = P(S = 1 X = x)$	posterior probability S
$e(x) = P(S = 1 X = x, Y = 1)$	propensity score function
$c = P(S = 1 Y = 1)$	labeling frequency
$h(x) = P(Y = 1 X = x, S = 0)$	conditional posterior probability of $Y = 1$ for unlabeled instance
β_*, γ_*	ground-truth parameters corresponding to $y(x)$ and $e(x)$
$\theta_* = (\beta_*, \gamma_*)$	vector containing all ground-truth parameters
$\sigma(t) = [1 + \exp(-t)]^{-1}$	sigmoid (logistic) activation function

2.2. Theoretical analysis for risk minimizers

In this section we discuss theoretical properties of minimizers of (5). We consider the estimator of θ_* , being a minimizer of (5) in the following sense:

$$\tilde{\theta} = \arg \min_{\theta: |\theta|_1 \leq w} Q_n(\theta), \quad (6)$$

where $w > 0$ is a radius of a ball around zero, in which we look for the optimal solution. The restriction to a ball with a radius w in (6) guarantees the existence of $\tilde{\theta}$, because Q_n is continuous. Clearly, one wants to take large w in (6) and such a choice will be justified by our theoretical results.

To be compatible with assumption $|\beta_*|_1 > |\gamma_*|_1$, we proceed as follows: first we calculate $|\tilde{\beta}|_1$ and $|\tilde{\gamma}|_1$ from (6). If $|\tilde{\beta}|_1 > |\tilde{\gamma}|_1$, then we let $\tilde{\theta} = (\tilde{\beta}, \tilde{\gamma})$, otherwise $\tilde{\theta} = (\tilde{\gamma}, \tilde{\beta})$.

Next, we impose some technical assumptions on the distribution of the feature vector that allow us to obtain theoretical results regarding the bounds for excess risk of our estimator. We assume throughout that components of X are linearly independent almost everywhere (a.e.), that is EXX^T is positive definite.

Assumption 2. We suppose that individual predictors X_{ij} 's are sub-Gaussian, i.e. there exists $\mu > 0$ such that for each $j = 1, \dots, p, i = 1, \dots, n$ and $t \in \mathbb{R}$ we have

$$\mathbb{E} \exp(tX_{ij}) \leq \exp(\mu^2 t^2 / 2).$$

A family of random variables having sub-Gaussian distributions is an important generalisation of a family of normally distributed random variables with mean zero. In this case μ^2 equals the variance of the corresponding variable. They can be described as variables such that their tail can be bounded by a tail of a certain normal variable $N(0, \sigma^2)$ up to a multiplicative constant. Apart from normally distributed variables the sub-Gaussian family includes e.g. all bounded random variables (for characterisation of such variables see e.g. Theorem 2.6 in [35]).

In [19] consistency in estimation of $\tilde{\theta}$ is established using classical techniques. In the current paper we apply much more sophisticated methods from the theory of empirical processes, which allow us to control the excess risk, or regret, of $\tilde{\theta}$ defined as

$$R(\tilde{\theta}) = Q(\tilde{\theta}) - Q(\theta_*).$$

Note that $R(\tilde{\theta})$ is interpreted as the amount by which the theoretical risk of $Q(\cdot)$ calculated at $\tilde{\theta}$ for a fixed data set deviates from its minimal value $Q(\theta_*)$ (see e.g. [36]). We note that minimiser $\tilde{\theta}$ is not necessarily unique and the obtained results will hold for any $\tilde{\theta}$ in (6).

In Theorem 1 we investigate properties of a minimiser of (5) over a neighborhood of the true parameter θ_*

$$\hat{\theta} = \arg \min_{\theta: |\theta - \theta_*|_1 \leq r} Q_n(\theta), \quad (7)$$

where $r > 0$ is an arbitrary number. Obviously, $\hat{\theta}$ cannot be found in practice, because its calculation requires knowledge of θ_* . However, risk consistency of the minimiser in (6) easily follows from the bound in Theorem 1. It will be established in Theorem 2.

Theorem 1. *Suppose Assumptions 1 and 2 hold. For each $s \in (0, 1)$ and any $\hat{\theta}$ defined in (7) we have*

$$P \left(R(\hat{\theta}) \leq \frac{32\mu r}{s} \sqrt{\frac{\log p}{n}} \right) \geq 1 - s. \quad (8)$$

Theorem 2. *Suppose Assumptions 1 and 2 hold. For any $\tilde{\theta}$ in (6) we have $R(\tilde{\theta}) \rightarrow 0$ in probability, if $\log p = o(n)$ and $w = C(n/\log p)^{1/2-\eta}$, where $C > 0$ is a constant and $0 < \eta < 1/2$.*

Proof of Theorem 2. Fix $\varepsilon > 0$. In Theorem 1 we take $r = C(n/\log p)^{1/2-\eta'}$ for $\eta' \in (0, \eta)$ and $s = \frac{32C\mu}{\varepsilon} \left(\frac{\log p}{n}\right)^{\eta'}$. Notice that $s \rightarrow 0$ for $n \rightarrow \infty$, because $\log p = o(n)$. Then for any $\hat{\theta}$ in (7)

$$P(R(\hat{\theta}) > \varepsilon) \leq s, \quad (9)$$

so this probability tends to zero as $n \rightarrow \infty$.

Let $K(\tau, r_0) := \{\theta : |\theta - \tau|_1 \leq r_0\}$ denote a ball with radius r_0 , centered at τ . For sufficiently large n we have $K(0, w) \subset K(\theta_*, (n/\log p)^{1/2-\eta'})$, because $\log p = o(n)$ and $w = C(n/\log p)^{1/2-\eta}$ for $\eta' < \eta$. Due to that the excess risk of any minimiser in (6) tends in probability to zero as well. \square

In Theorem 2 we establish that the excess risk of $\tilde{\theta}$ in (6) tends to zero even if the radius w tends to infinity as $n \rightarrow \infty$. The rate of w depends on a relation between $\log p$ and n , but also on the value $\eta \in (0, 1/2)$. As can be

observed in the proof of Theorem 2, the value η is a balance between a length of the radius w and a rate that probability (9) tends to zero. Smaller η allows for larger w to be taken in (6) but this in turn slows down the rate of convergence of the probability in (9).

In the proof of Theorem 1 we will need the following lemma, which is an extended version of the recent result from [37]. The latter is a multivariate version of the Concentration Principle [38, Theorem 4.12].

Lemma 1. *Let z_1, \dots, z_n be fixed elements from some set \mathcal{Z} . Moreover, let \mathcal{F} be a family of K -dimensional functions on \mathcal{Z} . Consider Lipschitz functions $h_i : \mathbb{R}^K \rightarrow \mathbb{R}, i = 1, \dots, n$ with a Lipschitz constant $L > 0$. If there exists $\bar{f} \in \mathcal{F}$ such that $h_i(\bar{f}(z_i)) = 0$ for $i = 1, \dots, n$, then*

$$\mathbb{E} \sup_{f \in \mathcal{F}} \left| \sum_{i=1}^n \varepsilon_i h_i(f(z_i)) \right| \leq 2\sqrt{2}L \mathbb{E} \sup_{f \in \mathcal{F}} \sum_{i=1}^n \sum_{k=1}^K \varepsilon_{i,k} f_k(z_i), \quad (10)$$

where $f = (f_1, f_2, \dots, f_K)$ for each $f \in \mathcal{F}$ and $\{\varepsilon_i\}_i, \{\varepsilon_{i,k}\}_{i,k}$ are independent Rademacher sequences.

The proof of Lemma 1 can be found in Appendix B.

Proof of Theorem 1. We take any $\hat{\theta}$ satisfying (7) and $s \in (0, 1)$. We also define a maximum deviation of a empirical process $Q_n(\theta) - Q(\theta)$:

$$U_n(r) = \sup_{|\theta - \theta_*|_1 \leq r} |J_n(\theta)|, \quad (11)$$

where $J_n(\theta) = Q_n(\theta) - Q_n(\theta_*) - Q(\theta) + Q(\theta_*)$. From the definition of $\hat{\theta}$ we have $Q_n(\hat{\theta}) \leq Q_n(\theta_*)$ and thus

$$0 \leq Q(\hat{\theta}) - Q(\theta_*) = -J_n(\hat{\theta}) + Q_n(\hat{\theta}) - Q_n(\theta_*) \leq U_n(r).$$

Therefore, we focus the attention on bounding (11).

We start with Markov's inequality, which gives $P(U_n(r) > z) \leq \mathbb{E}U_n(r)/z$ for any $z > 0$. The choice of z will be given later. Consequently, the main part of the proof is to bound $\mathbb{E}U_n(r)$, which is done using tools from the empirical process theory. Some of them are well-known, but we also need to apply some recent methods from [37].

The first step is the Symmetrization Lemma [39, Lemma 2.3.1], which implies that

$$\mathbb{E}U_n(r) \leq 2\mathbb{E} \sup_{|\theta - \theta_*|_1 \leq r} \left| \frac{1}{n} \sum_{i=1}^n \varepsilon_i [\phi(\beta^T X_i, \gamma^T X_i, S_i) - \phi(\beta_*^T X_i, \gamma_*^T X_i, S_i)] \right|, \quad (12)$$

where $\varepsilon_1, \dots, \varepsilon_n$ is a Rademacher sequence containing independent sign variables, i.e. $P(\varepsilon_i = 1) = P(\varepsilon_i = -1) = 0.5$. This sequence is also independent of vectors (X_i, Y_i, S_i) .

In order to handle the bound in (12), one usually applies the Contraction Principle [38, Theorem 4.12]. However, here we need a multivariate version of this result established in Lemma 1. In order to apply it, we first fix (X_i, S_i) and consider randomness only with respect to ε_i . Next, we apply a two-dimensional version of Lemma 1 with $f_{\beta, \gamma}(x) = ((\beta - \beta_*)^T x, (\gamma - \gamma_*)^T x)$ and functions $h_i, i = 1, \dots, n$ defined as

$$h_i(a, b) = \phi(\beta_*^T x_i + a, \gamma_*^T x_i + b, S_i) - \phi(\beta_*^T x_i, \gamma_*^T x_i, S_i),$$

where x_i and s_i are fixed values of X_i and S_i , respectively. It is easily checked that each h_i is Lipschitz with the Lipschitz constant $\sqrt{2}$, moreover $h_i(f_{\beta_*, \gamma_*}) = 0$. Therefore, in view of Lemma 1 we can bound (12) by

$$(8/n) \mathbb{E} \sup_{|\theta - \theta_*|_1 \leq r} \sum_{i=1}^n [\varepsilon_{i,1}(\beta - \beta_*)^T X_i + \varepsilon_{i,2}(\gamma - \gamma_*)^T X_i], \quad (13)$$

where $\varepsilon_{i,1}, \varepsilon_{i,2}$ are two independent Rademacher sequences defined in Lemma 1. Notice that the expected value in (13) is again considered with respect to ε_i and X_i . Obviously, we have

$$\sum_{i=1}^n \varepsilon_{i,1}(\beta - \beta_*)^T X_i \leq |\beta - \beta_*|_1 \sum_{i=1}^n \varepsilon_{i,1} X_i \leq r \sum_{i=1}^n \varepsilon_{i,1} X_i,$$

so we can bound (13) by $(16r/n) \mathbb{E} |\sum_{i=1}^n \varepsilon_{i,1} X_i|_\infty$. Next, we use **Assumption 1**, i.e. the fact that X_{ij} are sub-Gaussian with a parameter μ , which implies that $\sum_{i=1}^n \varepsilon_{i,1} X_{ij}$ is sub-Gaussian with a parameter $\sqrt{n}\mu$. Therefore, using Lemma 2.2 in [40] we obtain $\mathbb{E} |\sum_{i=1}^n \varepsilon_{i,1} X_i|_\infty \leq 2\mu\sqrt{n \log p}$, which implies that $\mathbb{E} U_n(r) \leq 32\mu r \sqrt{\log p/n}$. Finally, we take $z = \frac{32\mu r}{s} \sqrt{\frac{\log p}{n}}$, which finishes the proof. \square

2.3. Proposed algorithm: JERM

Estimator, defined in (6) has desirable theoretical properties, but its use in practice is problematic. This is due to the fact that in order to ensure uniqueness of the minimiser of the risk we have to impose additional assumption $|\beta^*|_1 > |\gamma^*|_1$, which is impossible to verify in practice, and therefore we are unable to distinguish between estimators of $y(x)$ and $e(x)$. To deal with this challenge, we propose a new, asymmetric procedure, called JERM (**J**oint **E**mpirical **R**isk **M**inimization) for optimizing the risk function described by (5) for which optimisation steps for the posterior and the propensity are different and the ensuing estimators are uniquely determined. The method alternately determines estimators for $y(x)$ and $e(x)$. We propose to estimate $e(x)$ using model fitted on the set \hat{P} which at each iteration is a new approximation of the set of positive examples $P = \{i : Y_i = 1\}$. Then, given an estimator of $e(x)$, we optimize function (5) with respect to β , which allows us to determine the estimator of $y(x)$. The whole procedure is described by Algorithm 1 and below we describe the details of the estimation of $e(x)$.

In order to estimate $e(x)$, we consider the theoretical risk function

$$H(\gamma) := -E_{X,S|Y=1} [S \log[\sigma(\gamma^T X)] + (1 - S) \log[1 - \sigma(\gamma^T X)]] . \quad (14)$$

The advantage of optimizing function $H(\cdot)$ compared to optimization of (4) is that the $H(\cdot)$ is convex with respect to its argument, which makes it possible to find a unique solution. The corresponding empirical risk function is

$$H_P(\gamma) = -\frac{1}{|P|} \sum_{i \in P} [S_i \log[\sigma(\gamma^T X_i)] + (1 - S_i) \log[1 - \sigma(\gamma^T X_i)]] . \quad (15)$$

As set P is unknown in PU setting, it has to be estimated. The proposed method for estimating the set P uses the technique of so-called 'spies'. By a spy we mean an observation belonging to unlabeled set $U = \{i : S_i = 0\}$,

which is the nearest neighbor of a certain observation from the labeled set $L = \{i : S_i = 1\}$. Note that here we deviate from the usual definition of spies which are defined as labeled examples added to the unlabeled dataset [33]. Formally, the set of spies is defined as $SP = \{i \in U : X_i = 1\text{-NN}(X_j), j \in L\}$. Intuitively, the spy set contains those unlabeled observations that are close to positive observations in a feature space, so they are also likely to be positive. Note, however, that apart from the set of spies, which will be assigned to \hat{P} , there may be other observations among unlabeled observations likely to be positive. Therefore, in addition, we consider observations for which the conditional probability $h(x) = P(Y = 1|X = x, S = 0)$ is larger than the value $h(x)$ for at least one spy. The rationale here is that we consider as plausible positives those elements which are as likely to be positive, in a specific sense, as at least one spy. We denote this set by $A = \{i \in U \setminus SP : h(X_i) > \min_{j \in SP} h(X_j)\}$. Probability $h(x)$ is unknown, however it can be expressed using the functions $e(x)$ and $y(x)$. Namely, denoting by $f(x)$ density of X , we have

$$h(x) = P(Y = 1|X = x, S = 0) = \frac{f(x)y(x)(1 - e(x))}{f(x)(1 - s(x))} = \frac{y(x)(1 - e(x))}{1 - y(x)e(x)}. \quad (16)$$

The function $h(x)$ can be estimated by plug-in the estimator $y(x)$ and the estimator $e(x)$ obtained in the previous iteration. In this way we obtain the estimator of set A (line 7 in Algorithm 1): $\hat{A} = \{i \in U \setminus SP : \hat{h}(X_i) > \min_{j \in SP} \hat{h}(X_j)\}$. Finally, the set of positive examples is estimated as $\hat{P} = L \cup SP \cup \hat{A}$. The whole procedure is shown as a flowchart in Figure 1, whereas Figure 2 visualises the process of determination of \hat{P} based on spies.

Algorithm 1: Joint Empirical Risk Minimization (JERM)

- 1: Input: training data $\mathcal{D} = \{(X_i, S_i) : i = 1, \dots, n\}$
- 2: Determine set of 'spies': $SP = \{i \in U : X_i = 1\text{-NN}(X_j), j \in L\}$.
- 3: Initialize $\hat{e}(X_i)$
- 4: **repeat**
- 5: Solve $\hat{\beta} = \arg \min_{\beta} Q_n(\beta, \hat{\gamma})$, where Q_n is defined in (5).
- 6: Calculate $\hat{y}(X_i) = \sigma(\hat{\beta}^T X_i)$, for $i = 1, \dots, n$.
- 7: Calculate

$$\hat{h}(X_i) = \frac{\hat{y}(X_i)(1 - \hat{e}(X_i))}{1 - \hat{y}(X_i)\hat{e}(X_i)}, \quad \hat{A} = \{i \in U \setminus SP : \hat{h}(X_i) > \min_{j \in SP} \hat{h}(X_j)\}$$

- 8: Determine set $\hat{P} = L \cup SP \cup \hat{A}$.
 - 9: Solve $\hat{\gamma} = \arg \min_{\gamma} H_{\hat{P}}(\gamma)$, where $H_P(\gamma)$ is defined in (15).
 - 10: Calculate $\hat{e}(X_i) = \sigma(\hat{\gamma}^T X_i)$, for $i = 1, \dots, n$.
 - 11: **until** convergence
-

The above algorithm contains some technical details that call for comments. First, as $Q_n(\beta, \gamma)$ is not convex in either β or γ , Majorisation-Minimisation (MM) algorithm (see e.g. [41], Section 5.8), commonly employed in such scenarios, is used to find the maximiser in line 5 in Algorithm 1. The analogous idea was used in previous papers

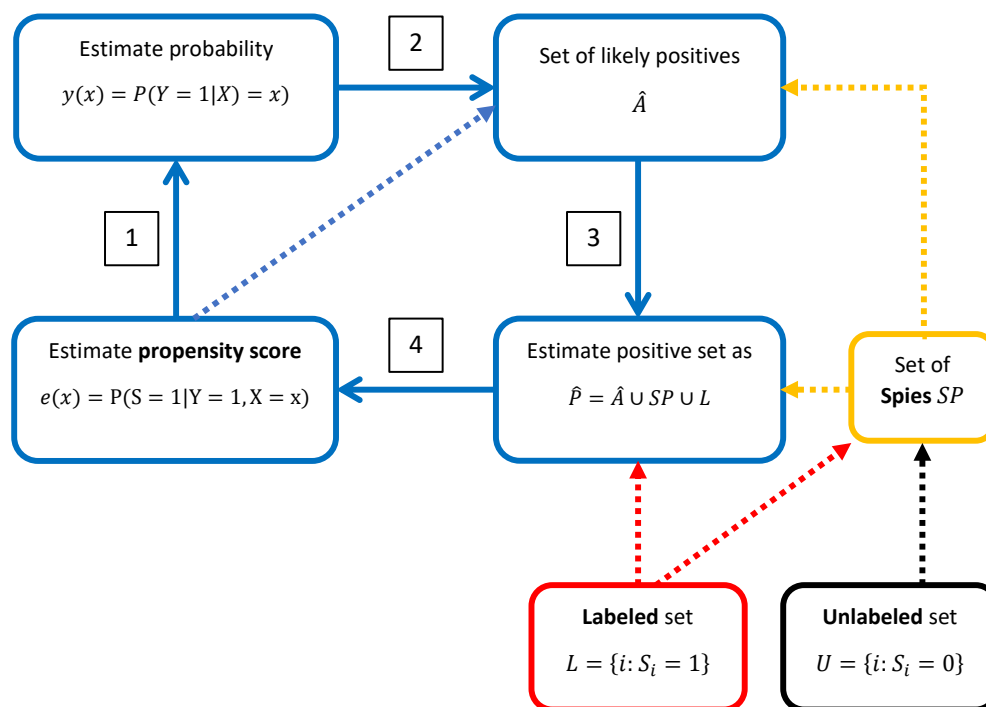


Figure 1: Flowchart of the proposed method JERM. (1) Given an estimator $e(x)$, we find $y(x)$ (line 5 in Algorithm 1). (2) Based on the estimators $y(x)$ and $e(x)$ and the set of spies, we determine the set of observations that are likely positive: \hat{A} . (3) The set of positive observations P is approximated by the sum of the sets \hat{A} , the set of spies and the set of positive observations. (4) \hat{P} is used for estimating $e(x)$ (line 9 in Algorithm 1).

on PU learning [34, 19], where it was shown that the use of the MM algorithm is superior to standard gradient-based algorithms. Secondly, we need to initialize the $e(x)$ estimator (line 3 in Algorithm 1). We use a simple estimator $\hat{e}(x) = 0.5(1 + \hat{s}(x))$, where $\hat{s}(x)$ is estimated by fitting the naive model in which variable S is treated as a class variable. The form of the estimator results from a simple inequality $s(x) = e(x)y(x) \leq e(x) \leq 1$ and considering the average value between $s(x)$ and 1.

3. Experiments

3.1. Methods and datasets

We use the most related methods discussed in the previous sections: PGLIN [18], LBE [17], SAR-EM [16] and TM [19]. Such methods were chosen because we focus on methods operating under the SAR assumption and those that directly estimate $e(x)$. To make the comparison fair, in all methods the base classifier is a logistic regression (LR). The LR model was also used as the base model in [17], [16] and [19]. The reference method is the NAIVE

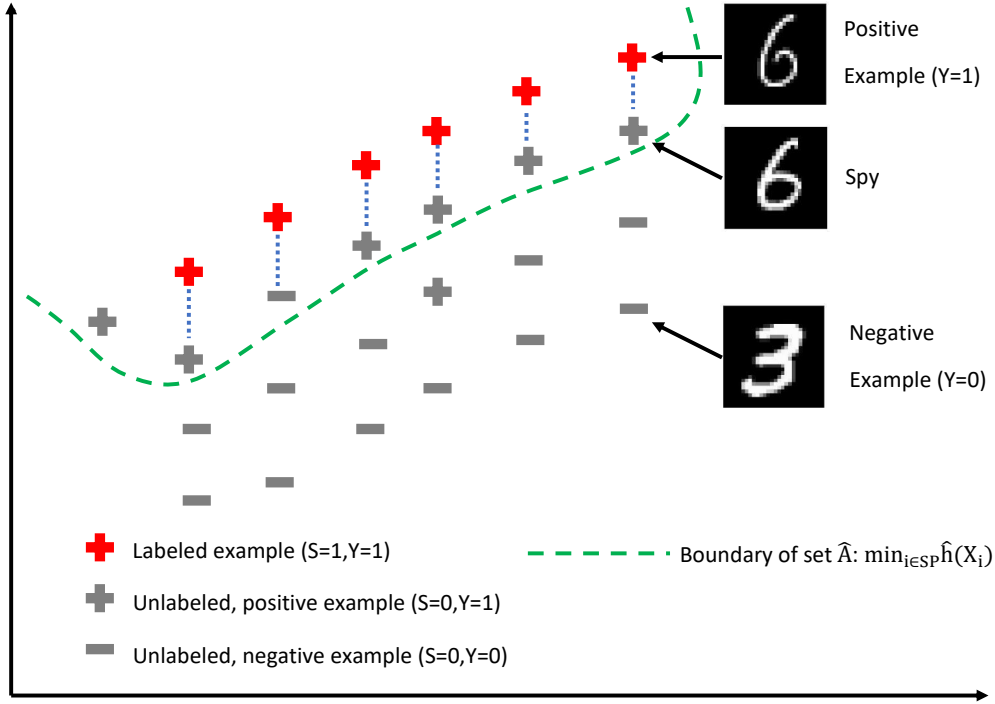


Figure 2: Visualization showing how to determine the set \hat{P} based on spies.

method, which uses the variable S as the unknown class variable, i.e. it treats unlabeled observations as negative. We also consider the ORACLE method, which assumes knowledge of the true variable Y . This method cannot be used in practice for PU data, but is useful in experiments because its result can be interpreted as yielding an upper bound on accuracy.

The experiments were conducted on 20 datasets, including 16 tabular datasets from the UCI repository and 4 image datasets: CIFAR10, MNIST, Fashion and USPS. The characteristics of the sets are provided in Table A.1 in Appendix A. Tabular datasets with multiple classes were transformed into binary classification datasets, such that the positive class includes the most common class, and the remaining classes are combined into the negative class. In the case of image datasets, we define the binary class variable depending on the particular dataset. In CIFAR10, all vehicles form a positive class and animals form a negative class. For MNIST, even and odd digits form the positive and negative classes, respectively. In the USPS positive digits less than five constitute the positive class, and remaining digits constitute the negative class. In FashionMNIST, clothing items worn on the upper body are marked as positive cases, the remaining images are in the negative class. For image data, we use a pre-trained deep neural network Resnet18 to extract the feature vector. For each image, the feature vector of dimension 512, is an outcome of the

average pooling layer. Then, the extracted feature vector is used by PU models.

3.2. Labelling strategies and evaluation methods

Given a set related to a binary classification problem, we artificially generate PU data using various labeling strategies. We assign all negative observations to the unlabeled set. From the positive observations we randomly select those that will be labeled with probability $e(x) = P(S = 1|X = x, Y = 1)$. We are considering the following strategies.

- S1.** Propensity score $e(x) = c$.
- S2.** Propensity score $e(x) = F_{\text{Logistic}}(x^T \beta^* + a)$.
- S3.** Propensity score $e(x) = F_{\text{Cauchy}}(x^T \beta^* + a)$.
- S4.** Propensity score $e(x) = [F_{\text{Logistic}}(x^T \beta^* + a)]^{10}$.

In the above formulas, F_{Logistic} and F_{Cauchy} denote the cumulative distribution functions of the logistic and Cauchy distributions, respectively. Parameter a is determined to control the value of labelling frequency $c = P(S = 1|Y = 1)$ and β^* is computed using ORACLE method with logistic regression. Strategy S1 corresponds to SCAR, whereas strategies S2-S4 correspond to SAR assumption. Moreover, note that S2 is related to assumption (2). The analysis of strategies S3 and S4 allows us to examine the robustness of the method to deviation from the assumption (2). The S4 strategy was considered in [17]. Note that in this case propensity score approximates 0-1 step function.

In the case of tabular datasets, we randomly split the data into a training set (75% of observations) and a test set (25% of observations). For image datasets, we use predefined splits provided in the PyTorch library [42]. From the training data, we generate PU data using the labeling strategies described above. Then, the PU models are fitted on training data. Finally, the models are evaluated on test data. We use balanced accuracy as the primary evaluation metric because this metric takes into account class imbalances that occur in some datasets. The above steps are repeated for 10 random data splits and finally we report the average values and standard deviations.

3.3. Discussion

The aim of the experiments was to address the following questions. (1) How do the considered methods work for different labeling schemes? (2) Is the proposed method JERM robust to deviations from model assumptions? (3) What is the effectiveness of the methods for different label frequencies?

3.3.1. Analysis of performance for different labeling schemes

Table 2 shows summary results of pairwise comparisons: wins (W), losses (L) and draws (D) of the proposed method JERM against each competitive method in terms of average balanced accuracy, whereas Tables A.2-A.13 in Appendix show detailed results for S1-S4 and labeling frequency $c = 0.3, 0.5, 0.7$.

When compared with the NAIVE method and SAR-EM, the proposed method JERM is the clear winner for most datasets, regardless of labeling scheme and label frequency. Comparison with LBE shows, that for most datasets, the classification accuracy is comparable, however in the case of S4, the proposed method works significantly better for 3-5 datasets, while the opposite situation does not happen. Note that the labeling strategy (S4) originates from [17], where LBE was proposed. Comparison with PGLIN reveals that for the strategies S2-S4, the JERM method has significantly higher accuracy for a larger number of datasets. The effectiveness of the TM method depends on the labeling scheme. For S1, TM performs similarly (12-14 datasets) or better (5-7 datasets) than the JERM method. The situation changes for non-SCAR schemes (S2-S4), where for most datasets the JERM works better or comparable to TM. Importantly, for S3 and S4, on no dataset TM performs better than the JERM method.

In addition, Table 3 shows percentage of absolute wins (averaged over c) of the JERM method against each competitive method. The proposed method JERM turns out to be a winner for most datasets and S2-S4 scenarios. In the case of S1, the JERM works better than the NAIVE and EM for most datasets.

The analysis of the average ranks for individual methods (last row in Tables 2-13) indicates that the JERM works on average most effectively for non-SCAR schemes and lower label frequencies ($c = 0.3$ and $c = 0.5$), while for $c = 0.7$ is the second best. For the SCAR scheme S1, the TM method emerges as the winner.

3.3.2. Robustness to deviations from model assumptions

Note that our method, as well as LBE, is based on the assumption (2) indicating that the propensity function depends on a linear combination of features through a sigmoidal activation function. The labeling schemes S1 and S2 satisfy this assumption, in contrast to S3 and S4 scenarios. In particular, for S4, the propensity function approximates 0-1 step function and deviates significantly from the assumed sigmoid function. Importantly, the JERM achieves the highest averaged ranks for S3 and S4 and lower label frequencies ($c = 0.3, 0.5$). This points to the robustness of our method when the propensity score does not follow logistic model. Additionally, for the S4 scheme, the JERM performs significantly better (3-5 datasets) or comparable (15-17 datasets) to LBE, which may indicate that the proposed method is more resistant to deviation from assumptions than LBE.

3.3.3. Performance for different labeling frequencies

The analysis of the situation of low label frequency c is particularly interesting, because in this situation, learning is usually based on small (or even extremely small) number of labelled instances. Experiments show that for low label frequency, the proposed method is more effective than other competitors. The JERM method turns out to be the winner (in terms of averaged ranks) for S2-S4 and is the second best for S1. This is confirmed by more detailed analyzes carried out on selected datasets (Segment, Banknote, CIFAR10, Fashion), for which we studied the dependence between balanced accuracy and the label frequency c (Figures 3 and 4). We observe high accuracy of the proposed method even for small label frequency, such as $c = 0.1$. In the case of some datasets and scenarios (e.g. the Segment dataset and the S4 scheme), the advantage is very pronounced. As expected, the performance of all

methods increases with c , approaching the effectiveness of the ORACLE method. For image datasets, the shapes of the accuracy curves corresponding to the JERM method and LBE are similar, which is understandable because both methods are based on a the same assumption (2). Importantly, however, the accuracy curve for the proposed method usually dominates the accuracy curve for LBE.

3.3.4. Computational issues

Finally, we briefly discuss computational issues. All considered methods based on alternating model fitting for a posterior probability and propensity score function (EM, LBE, TM) are quite computationally expensive. In the case of the proposed method, the computational cost is additionally increased by the use of the MM algorithm in optimization and determination of spies. However, despite this, the computation times are comparable to the most related LBE method. For example, for CIFAR10 data and scheme S1, the computation time for LBE is 133.01 secs, while the computation time for the proposed method is slightly less 120.23. In turn, for MNIST data and scheme S1, the computation time for LBE is 164.15 and is slightly smaller than the computation time for JERM which is 178.00 secs.

Table 2: Wins (W), losses (L) and draws (D) of the proposed method JERM against each competitive method in terms of average balanced accuracy. Win/Loss means that the difference in average accuracy is greater/smaller for the proposed method and intervals $\text{mean} \pm \text{sd}$ for the pair of compared methods do not overlap. A draw (D) means that the intervals $\text{mean} \pm \text{sd}$ for the pair of compared methods overlap.

Strategy	c	NAIVE			EM			LBE			PGLIN			TM		
		W	L	D	W	L	D	W	L	D	W	L	D	W	L	D
S1	0.3	19	0	1	17	0	3	1	1	18	8	2	10	3	5	12
	0.5	18	0	2	11	0	9	2	2	16	3	6	11	1	5	14
	0.7	13	2	5	8	6	6	3	2	15	1	8	11	1	7	12
S2	0.3	20	0	0	18	0	2	3	1	16	13	0	7	14	0	6
	0.5	18	0	2	16	0	4	4	2	14	9	1	10	14	0	6
	0.7	15	0	5	11	1	8	3	1	16	5	3	12	11	1	8
S3	0.3	20	0	0	18	0	2	1	2	17	13	2	5	9	0	11
	0.5	17	0	3	14	0	6	2	1	17	7	2	11	9	0	11
	0.7	12	0	8	10	0	10	1	1	18	5	4	11	8	0	12
S4	0.3	19	0	1	18	0	2	3	0	17	11	0	9	15	0	5
	0.5	17	0	3	15	0	5	5	0	15	10	1	9	13	0	7
	0.7	14	0	6	10	1	9	3	0	17	5	2	13	10	0	10

Table 3: Percentage of absolute wins (averaged over c) of the JERM method against each competitive method.

Strategy	NAIVE	EM	LBE	PGLIN	TM
S1	0.91	0.8	0.42	0.48	0.42
S2	0.95	0.9	0.63	0.71	0.87
S3	0.97	0.87	0.62	0.65	0.8
S4	0.97	0.9	0.65	0.77	0.87

4. Conclusions

In this work, we proposed a novel PU learning method JERM, based on joint modeling the posterior probability and the propensity score using sigmoid functions which depend on the linear combination of features. The parameters of the above functions are estimated by optimizing the joint risk function for the observed label indicator. The risk function minimizer was analyzed theoretically. In particular, we established risk consistency for the empirical risk minimizer.

We also proposed an iterative method for optimizing joint empirical risk. The algorithm consists in alternately determining estimates for the posterior probability and the propensity score function. An innovative element of the work is the use of the spies technique to estimate the set of positive observations, which in turn enables the determination of the propensity score estimator. Importantly, in future research, the proposed propensity score estimator can be combined with other PU methods that require knowledge of the propensity scores. The results of experiments conducted on 20 real data sets indicate that the proposed method works comparable to or better than state-of-the-art methods based on propensity score estimation. The advantage of our method is especially noticeable when the SCAR assumption is not met and the labeling frequency is low. Moreover, we have shown that the method is robust with respect to the form of labeling. Interesting future research direction is investigation of effectiveness of selecting active predictors under the considered scenario by augmenting joint empirical risk considered here with sparsity-inducing regularizers.

References

- [1] J. Bekker, J. Davis, Learning from positive and unlabeled data: a survey, *Machine Learning* 109 (2020) 719–760.
- [2] O. Chapelle, B. Schölkopf, A. Zien, *Semi-Supervised Learning*, The MIT Press, 2010.
- [3] J. W. Park, M. K. Chu, J. M. Kim, S. G. Park, S. J. Cho, Analysis of trigger factors in episodic migraineurs using a smartphone headache diary applications, *PloS one* 11 (2) (2016) 1–13.
- [4] X. Li, B. Liu, Learning to classify texts using positive and unlabeled data, in: *Proceedings of the 18th International Joint Conference on Artificial Intelligence, IJCAI’03, 2003*, p. 587–592.
- [5] G. P. C. Fung, J. X. Yu, H. Lu, P. S. Yu, Text classification without negative examples revisit, *IEEE Transactions on Knowledge and Data Engineering* 18 (1) (2006) 6–20.

- [6] F. Chiaroni, M.-C. Rahal, N. Hueber, F. Dufaux, Learning with a generative adversarial network from a positive unlabeled dataset for image classification, in: Proceedings of the 25th IEEE International Conference on Image Processing, ICIP'18, 2018, pp. 1–6.
- [7] Y. Luo, S. Cheng, C. Liu, F. Jiang, Pu-learning in payload-based web anomaly detection, in: Proceedings of the Third Conference on Security of Smart Cities, industrial Control Systems and Communications, SSIC'2018, 2018, pp. 1–5.
- [8] E. Shultheis, R. Babbar, M. Wydmuch, K. Dembczyński, On missing labels, long-tails and propensities in extreme multi-label classification, in: KDD'22, 2022, pp. 1547–1557.
- [9] F. Li, S. Dong, A. Leier, M. Han, X. Guo, J. Xu, X. Wang, S. Pan, C. Jia, Y. Zhang, G. Webb, L. J. M. Coin, C. Li, J. Song, Positive-unlabeled learning in bioinformatics and computational biology: a brief review, *Briefings in Bioinformatics* 23 (1) (2021).
- [10] C. Elkan, The foundations of cost-sensitive learning, in: Proceedings of the seventeenth international joint conference on artificial intelligence, Vol. 17, Lawrence Erlbaum Associates Ltd, 2001, pp. 973–978.
- [11] C. Elkan, K. Noto, Learning classifiers from only positive and unlabeled data, in: Proceedings of the 14th ACM SIGKDD International Conference on Knowledge Discovery and Data Mining, KDD '08, 2008, pp. 213–220.
- [12] H. Ramaswamy, C. Scott, A. Tewari, Mixture proportion estimation via kernel embeddings of distributions, in: Proceedings of The 33rd International Conference on Machine Learning, Vol. 48, 2016, pp. 2052–2060.
- [13] J. Bekker, J. Davis, Estimating the class prior in positive and unlabeled data through decision tree induction, in: Proceedings of the 32th AAAI Conference on Artificial Intelligence, 2018, pp. 1–8.
- [14] P. Teisseyre, J. Mielniczuk, M. Łazicka, Different strategies of fitting logistic regression for positive and unlabelled data, in: Proceedings of International Conference on Computational Science, ICCS'20, 2020, pp. 1–14.
- [15] P. Teisseyre, Classifier chains for positive unlabelled multi-label learning, *Knowledge-Based Systems* 213 (2021) 106709.
- [16] J. Bekker, P. Robberechts, J. Davis, Beyond the Selected Completely At Random Assumption for Learning from Positive and Unlabeled Data, in: Proceedings of the 2019 European Conference on Machine Learning and Principles and Practice of Knowledge Discovery in Databases, ECML'19, 2019, pp. 71–85.
- [17] C. Gong, Q. Wang, T. Liu, B. Han, J. You, J. Yang, D. Tao, Instance-dependent positive and unlabeled learning with labeling bias estimation, *IEEE Trans Pattern Anal Mach Intell* (2021) 1–16.
- [18] W. Gerych, T. Hartvigsen, L. Buquicchio, E. Agu, E. Rundensteiner, Recovering the propensity score from biased positive unlabeled data, in: Proceedings of the AAAI Conference on Artificial Intelligence, AAAI'22, 2022, pp. 6694–6702.
- [19] K. Furmańczyk, J. Mielniczuk, W. Rejchel, P. Teisseyre, Double logistic regression approach to biased positive-unlabeled data, in: Proceedings of the European Conference on Artificial Intelligence, ECAI'23, 2023, pp. 764–771.
- [20] B. Na, H. Kim, K. Song, W. Joo, Y.-Y. Kim, I. Moon, Deep generative positive-unlabeled learning under selection bias, in: Proceedings of CIKM'20, ACM, New York, NY, USA, 2020, pp. 1155–1164.
- [21] A. Wawrzęczyk, J. Mielniczuk, One-class classification approach to variational learning from biased positive unlabelled data, in: Proceedings of the European Conference on Artificial Intelligence, ECAI'23, 2023, pp. 1720–1727.
- [22] A. Menon, B. Rooyen, N. Natarajan, Learning from binary labels with instance-dependent noise, *Machine Learning* (2018) 1561–1595.
- [23] T. Cannings, Y. Fan, R. Samworth, Classification with imperfect training labels, *Biometrika* (2020) 311–330.
- [24] C. Gong, M. I. Zulfiqar, C. Zhang, S. Mahmood, J. Yang, A recent survey on instance-dependent positive and unlabeled learning, *Fundamental Research* (2022).
- [25] F. He, T. Liu, J. Webb, D. Tao, [Instance-dependent pu learning by Bayesian optimal relabeling](#), manuscript (2018).
URL [arXiv:180802180](https://arxiv.org/abs/180802180)
- [26] O. Coudray, C. Keribin, P. Massart, P. Pamphile, Risk bounds for positive-unlabeled learning under the selected at random assumption, *Journal of Machine Learning Research* (2023) 1–31.
- [27] M. C. du Plessis, G. Niu, M. Sugiyama, Analysis of learning from positive and unlabeled data, in: Proceedings of the International Conference on Neural Information Processing Systems, NIPS'14, 2014, pp. 703–711.
- [28] R. Kiryo, G. Niu, M. C. du Plessis, M. Sugiyama, Positive-unlabeled learning with non-negative risk estimator, in: Proceedings of the

- International Conference on Neural Information Processing Systems, NIPS'17, 2017, pp. 1674–1684.
- [29] H. Chen, F. Liu, Y. Wang, L. Zhao, H. Wu, A variational approach for learning from positive and unlabeled data, in: Proceedings of the International Conference on Neural Information Processing Systems, NIPS'20, 2020, pp. 14844–14854.
- [30] Y. Zhao, Q. Xu, Y. Jiang, P. Wen, Q. Huang, Dist-pu: Positive-unlabeled learning from a label distribution perspective, in: Proceedings of the Conference on Computer Vision and Pattern Recognition, CVPR'22, 2022, pp. 14461–14470.
- [31] Y. Liu, J. Zhao, Y. Xu, Robust and unbiased positive and unlabeled learning, *Knowledge-Based Systems* 277 (2023) 1–15.
- [32] H. Song, G. Raskutti, Pu-lasso: high-dimensional variable selection with presence-only data, *Journal of American Statistical Association* 115 (2019) 334–347.
- [33] B. Liu, W. S. Lee, P. S. Yu, X. Li, Partially supervised classification of text documents, in: Proceedings of the 19-th International Conference on Machine Learning, ICLM'02, 2002, pp. 387–394.
- [34] M. Łazicka, J. Mielniczuk, P. Teisseyre, Estimating the class prior for positive and unlabelled data via logistic regression, *Advances in Data Analysis and Classification* 15 (2021) 1039–1068.
- [35] M. Wainwright, *High-dimensional Statistics*, Cambridge University Press, 2019.
- [36] M. Reid, R. Williamson, Information divergence and risk for binary experiments, *Journal of Machine Learning Research* 12 (2011) 731–817.
- [37] A. Maurer, A vector-contraction inequality for Rademacher complexities, in: *Algorithmic Learning Theory, ALT'16*, 2016, pp. 3–17.
- [38] M. Ledoux, M. Talagrand, *Probability in Banach Spaces: Isoperimetry and Processes*, Springer, Berlin, 1991.
- [39] A. v. d. Vaart, *Asymptotic Statistics*, Cambridge University Press, Cambridge, 1998.
- [40] L. Devroye, G. Lugosi, *Combinatorial Methods in Density Estimation*, Springer, New York, 2012.
- [41] T. Hastie, R. Tibshirani, M. Wainwright, *Statistical Learning with Sparsity: The Lasso and Generalizations*, CRC, London, 2015.
- [42] A. Paszke, S. Gross, F. Massa, A. Lerer, J. Bradbury, G. Chanan, T. Killeen, Z. Lin, N. Gimelshein, L. Antiga, A. Desmaison, A. Kopf, E. Yang, Z. DeVito, M. Raison, A. Tejani, S. Chilamkurthy, B. Steiner, L. Fang, J. Bai, S. Chintala, Pytorch: An imperative style, high-performance deep learning library, in: *Advances in Neural Information Processing Systems, NIPS'19*, 2019, pp. 8024–8035.

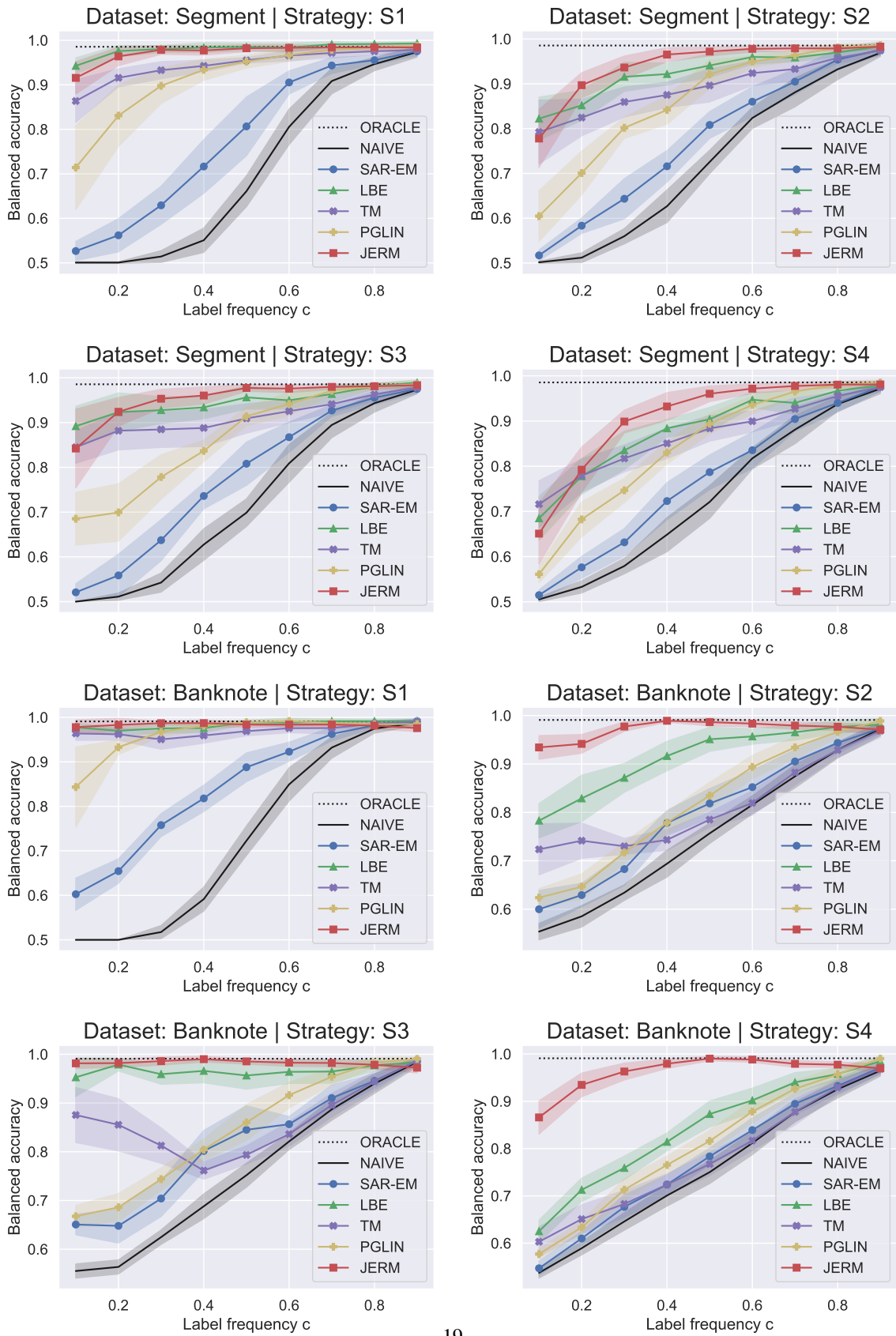


Figure 3: Balanced accuracy with respect to label frequency c for selected tabular datasets and strategies S1-S4.

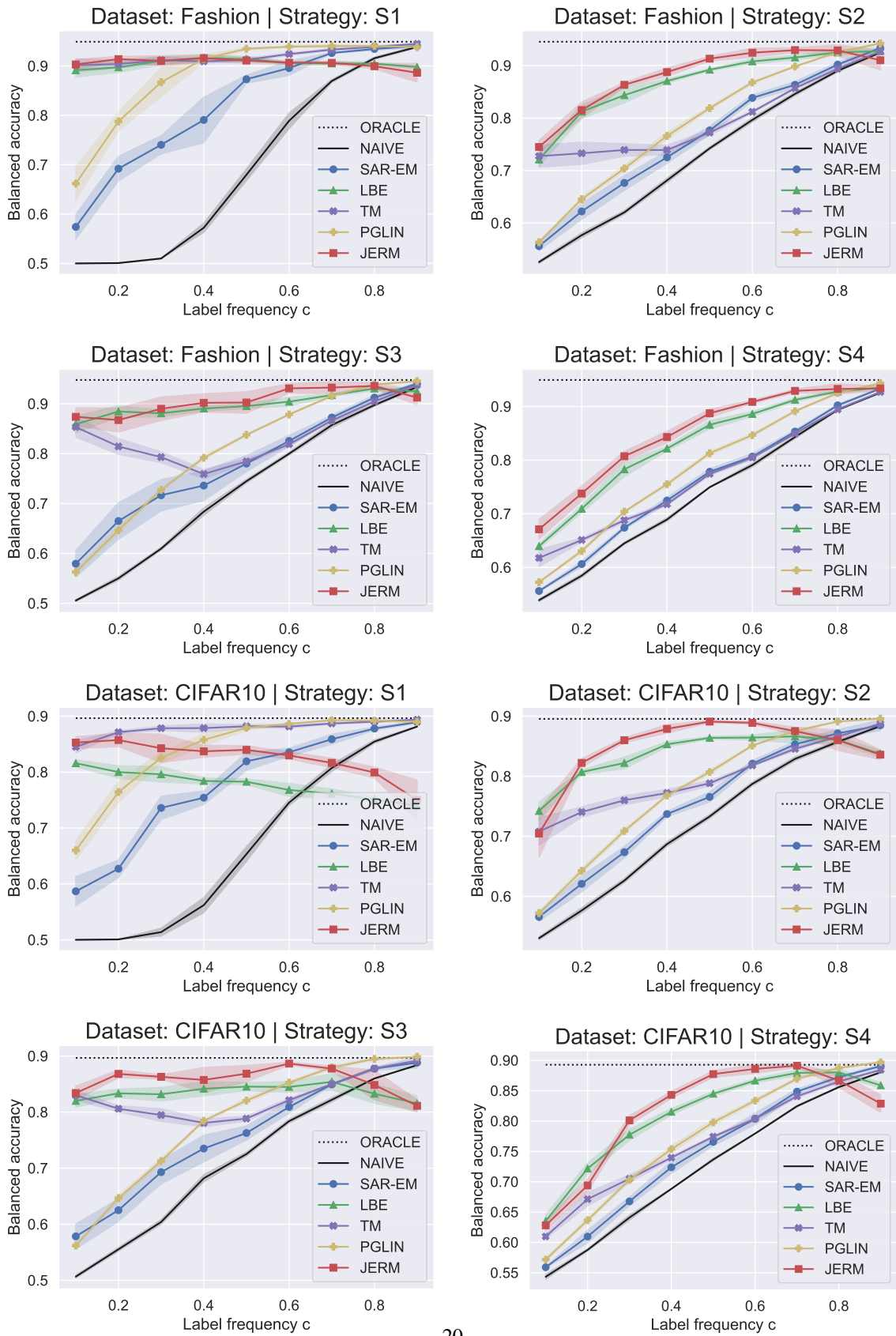


Figure 4: Balanced accuracy with respect to label frequency c for selected image datasets and strategies S1-S4.

Appendix A.

Table A.1: Statistics of the considered data sets.

Dataset	n	p	$P(Y = 1)$	positives	type
Breast-w	699	9	0.34	241.0	tabular
Diabetes	768	8	0.35	268.0	tabular
Spambase	4601	57	0.39	1813.0	tabular
Wdbc	569	30	0.37	212.0	tabular
Banknote	1372	4	0.44	610.0	tabular
Heart	270	13	0.44	120.0	tabular
Ionosphere	351	34	0.64	225.0	tabular
Sonar	208	60	0.53	111.0	tabular
Haberman	306	3	0.26	81.0	tabular
Segment	2310	19	0.14	330.0	tabular
Waveform	5000	40	0.34	1692.0	tabular
Yeast	1484	8	0.31	463.0	tabular
Musk	6598	166	0.15	1017.0	tabular
Isolet	7797	617	0.04	300.0	tabular
Semeion	1593	256	0.1	162.0	tabular
Vehicle	846	18	0.26	218.0	tabular
CIFAR10	50000	-	0.4	20000	images
MNIST	60000	-	0.49	29492	images
USPS	7291	-	0.58	4240	images
Fashion	60000	-	0.5	30000	images

Appendix A.1. Results for labeling strategy S1

Table A.2: Balanced accuracy for datasets, for labelling strategy S1 and $c = 0.3$.

Dataset	ORACLE	NAIVE	SAR-EM	LBE	PGLIN	TM	JERM
Breast-w	0.952 ± 0.017	0.529 ± 0.022	0.74 ± 0.042	0.906 ± 0.036	0.868 ± 0.022	0.904 ± 0.016	0.889 ± 0.028
Diabetes	0.716 ± 0.026	0.501 ± 0.002	0.519 ± 0.017	0.636 ± 0.03	0.717 ± 0.02	0.687 ± 0.064	0.684 ± 0.026
Spambase	0.894 ± 0.009	0.512 ± 0.005	0.673 ± 0.017	0.863 ± 0.016	0.672 ± 0.035	0.883 ± 0.008	0.813 ± 0.031
Wdbc	0.971 ± 0.01	0.565 ± 0.036	0.693 ± 0.049	0.859 ± 0.035	0.735 ± 0.042	0.904 ± 0.036	0.753 ± 0.078
Banknote	0.991 ± 0.005	0.519 ± 0.009	0.759 ± 0.024	0.974 ± 0.01	0.959 ± 0.027	0.964 ± 0.016	0.983 ± 0.007
Heart	0.808 ± 0.038	0.512 ± 0.014	0.6 ± 0.07	0.683 ± 0.073	0.774 ± 0.029	0.771 ± 0.046	0.657 ± 0.052
Ionosphere	0.82 ± 0.022	0.5 ± 0.007	0.508 ± 0.048	0.664 ± 0.081	0.792 ± 0.047	0.784 ± 0.052	0.726 ± 0.05
Sonar	0.778 ± 0.051	0.502 ± 0.005	0.533 ± 0.045	0.684 ± 0.082	0.607 ± 0.069	0.616 ± 0.055	0.574 ± 0.093
Haberman	0.511 ± 0.019	0.5 ± 0.0	0.499 ± 0.003	0.532 ± 0.045	0.511 ± 0.019	0.502 ± 0.005	0.573 ± 0.064
Segment	0.985 ± 0.006	0.515 ± 0.013	0.614 ± 0.035	0.98 ± 0.008	0.861 ± 0.055	0.932 ± 0.023	0.979 ± 0.008
Waveform	0.841 ± 0.015	0.511 ± 0.004	0.691 ± 0.026	0.833 ± 0.009	0.729 ± 0.023	0.84 ± 0.011	0.82 ± 0.012
Yeast	0.518 ± 0.01	0.5 ± 0.0	0.501 ± 0.002	0.623 ± 0.021	0.536 ± 0.024	0.576 ± 0.032	0.658 ± 0.019
Musk	0.761 ± 0.012	0.512 ± 0.011	0.565 ± 0.018	0.83 ± 0.014	0.685 ± 0.022	0.805 ± 0.016	0.833 ± 0.014
Isolet	0.62 ± 0.03	0.5 ± 0.0	0.569 ± 0.032	0.897 ± 0.009	0.645 ± 0.035	0.85 ± 0.029	0.896 ± 0.027
Semeion	0.819 ± 0.029	0.504 ± 0.009	0.569 ± 0.052	0.851 ± 0.039	0.808 ± 0.049	0.851 ± 0.02	0.836 ± 0.022
Vehicle	0.937 ± 0.017	0.527 ± 0.021	0.671 ± 0.054	0.904 ± 0.022	0.799 ± 0.059	0.844 ± 0.033	0.878 ± 0.08
CIFAR10	0.893 ± 0.0	0.512 ± 0.003	0.726 ± 0.031	0.808 ± 0.011	0.822 ± 0.018	0.88 ± 0.002	0.849 ± 0.007
MNIST	0.858 ± 0.0	0.51 ± 0.003	0.606 ± 0.019	0.787 ± 0.016	0.795 ± 0.018	0.749 ± 0.024	0.767 ± 0.007
USPS	0.877 ± 0.0	0.505 ± 0.0	0.666 ± 0.021	0.775 ± 0.005	0.812 ± 0.03	0.83 ± 0.007	0.778 ± 0.01
Fashion	0.948 ± 0.0	0.509 ± 0.003	0.766 ± 0.009	0.906 ± 0.009	0.872 ± 0.021	0.913 ± 0.004	0.907 ± 0.008
Avg. rank	0.0	1.05	2.0	4.8	3.8	4.8	4.55

Table A.3: Balanced accuracy for datasets, for labelling strategy S1 and $c = 0.5$.

Dataset	ORACLE	NAIVE	SAR-EM	LBE	PGLIN	TM	JERM
Breast-w	0.952 ± 0.017	0.662 ± 0.043	0.851 ± 0.023	0.949 ± 0.024	0.909 ± 0.021	0.915 ± 0.024	0.948 ± 0.035
Diabetes	0.716 ± 0.026	0.51 ± 0.016	0.575 ± 0.027	0.639 ± 0.03	0.732 ± 0.026	0.715 ± 0.036	0.663 ± 0.027
Spambase	0.894 ± 0.009	0.605 ± 0.016	0.756 ± 0.017	0.858 ± 0.014	0.843 ± 0.02	0.889 ± 0.01	0.778 ± 0.013
Wdbc	0.971 ± 0.01	0.686 ± 0.054	0.789 ± 0.066	0.903 ± 0.04	0.873 ± 0.03	0.918 ± 0.029	0.863 ± 0.037
Banknote	0.991 ± 0.005	0.736 ± 0.038	0.884 ± 0.019	0.989 ± 0.007	0.986 ± 0.01	0.97 ± 0.016	0.984 ± 0.006
Heart	0.808 ± 0.038	0.618 ± 0.047	0.717 ± 0.042	0.682 ± 0.066	0.77 ± 0.04	0.783 ± 0.042	0.684 ± 0.083
Ionosphere	0.82 ± 0.022	0.558 ± 0.046	0.721 ± 0.067	0.69 ± 0.046	0.794 ± 0.03	0.818 ± 0.051	0.733 ± 0.038
Sonar	0.778 ± 0.051	0.534 ± 0.041	0.643 ± 0.069	0.713 ± 0.056	0.642 ± 0.063	0.687 ± 0.055	0.616 ± 0.072
Haberman	0.511 ± 0.019	0.5 ± 0.0	0.51 ± 0.018	0.541 ± 0.029	0.513 ± 0.035	0.508 ± 0.028	0.563 ± 0.052
Segment	0.985 ± 0.006	0.648 ± 0.038	0.816 ± 0.058	0.989 ± 0.006	0.951 ± 0.017	0.954 ± 0.014	0.982 ± 0.009
Waveform	0.841 ± 0.015	0.584 ± 0.017	0.74 ± 0.03	0.835 ± 0.006	0.825 ± 0.013	0.846 ± 0.007	0.817 ± 0.011
Yeast	0.518 ± 0.01	0.5 ± 0.0	0.511 ± 0.006	0.619 ± 0.014	0.588 ± 0.044	0.622 ± 0.015	0.651 ± 0.021
Musk	0.761 ± 0.012	0.55 ± 0.01	0.623 ± 0.023	0.799 ± 0.009	0.734 ± 0.021	0.811 ± 0.019	0.821 ± 0.013
Isolet	0.62 ± 0.03	0.516 ± 0.01	0.609 ± 0.032	0.899 ± 0.012	0.685 ± 0.024	0.862 ± 0.031	0.909 ± 0.017
Semeion	0.819 ± 0.029	0.555 ± 0.042	0.637 ± 0.026	0.89 ± 0.027	0.835 ± 0.018	0.842 ± 0.024	0.86 ± 0.016
Vehicle	0.937 ± 0.017	0.614 ± 0.033	0.776 ± 0.052	0.928 ± 0.014	0.901 ± 0.027	0.877 ± 0.023	0.907 ± 0.05
CIFAR10	0.893 ± 0.0	0.655 ± 0.012	0.809 ± 0.008	0.775 ± 0.012	0.875 ± 0.003	0.879 ± 0.004	0.824 ± 0.007
MNIST	0.858 ± 0.0	0.625 ± 0.01	0.738 ± 0.021	0.765 ± 0.01	0.847 ± 0.002	0.832 ± 0.003	0.755 ± 0.005
USPS	0.877 ± 0.0	0.645 ± 0.008	0.791 ± 0.014	0.772 ± 0.009	0.864 ± 0.002	0.849 ± 0.005	0.78 ± 0.011
Fashion	0.948 ± 0.0	0.675 ± 0.008	0.861 ± 0.017	0.921 ± 0.005	0.932 ± 0.002	0.914 ± 0.003	0.905 ± 0.004
Avg. rank	0.0	1.0	2.45	4.45	4.25	4.7	4.15

Table A.4: Balanced accuracy for datasets, for labelling strategy **S1** and $c = 0.7$.

Dataset	ORACLE	NAIVE	SAR-EM	LBE	PGLIN	TM	JERM
Breast-w	0.952 ± 0.017	0.846 ± 0.014	0.9 ± 0.017	0.959 ± 0.022	0.94 ± 0.017	0.919 ± 0.023	0.95 ± 0.016
Diabetes	0.716 ± 0.026	0.581 ± 0.021	0.675 ± 0.029	0.634 ± 0.025	0.75 ± 0.011	0.719 ± 0.036	0.665 ± 0.03
Spambase	0.894 ± 0.009	0.757 ± 0.021	0.83 ± 0.012	0.846 ± 0.01	0.895 ± 0.006	0.895 ± 0.008	0.795 ± 0.022
Wdbc	0.971 ± 0.01	0.818 ± 0.048	0.855 ± 0.039	0.919 ± 0.019	0.923 ± 0.028	0.938 ± 0.02	0.872 ± 0.059
Banknote	0.991 ± 0.005	0.935 ± 0.024	0.958 ± 0.016	0.991 ± 0.006	0.988 ± 0.005	0.98 ± 0.014	0.985 ± 0.006
Heart	0.808 ± 0.038	0.753 ± 0.038	0.791 ± 0.031	0.704 ± 0.064	0.804 ± 0.04	0.792 ± 0.04	0.714 ± 0.034
Ionosphere	0.82 ± 0.022	0.801 ± 0.045	0.831 ± 0.034	0.719 ± 0.063	0.794 ± 0.041	0.826 ± 0.036	0.766 ± 0.037
Sonar	0.778 ± 0.051	0.653 ± 0.055	0.693 ± 0.065	0.722 ± 0.084	0.649 ± 0.044	0.74 ± 0.034	0.641 ± 0.067
Haberman	0.511 ± 0.019	0.499 ± 0.003	0.515 ± 0.025	0.51 ± 0.012	0.509 ± 0.015	0.514 ± 0.034	0.552 ± 0.028
Segment	0.985 ± 0.006	0.906 ± 0.04	0.934 ± 0.016	0.992 ± 0.004	0.98 ± 0.009	0.972 ± 0.009	0.984 ± 0.006
Waveform	0.841 ± 0.015	0.713 ± 0.014	0.782 ± 0.012	0.836 ± 0.006	0.865 ± 0.01	0.851 ± 0.012	0.808 ± 0.014
Yeast	0.518 ± 0.01	0.501 ± 0.002	0.526 ± 0.018	0.604 ± 0.022	0.599 ± 0.041	0.627 ± 0.015	0.642 ± 0.015
Musk	0.761 ± 0.012	0.638 ± 0.016	0.695 ± 0.018	0.789 ± 0.007	0.786 ± 0.016	0.816 ± 0.013	0.81 ± 0.021
Isolet	0.62 ± 0.03	0.547 ± 0.015	0.647 ± 0.029	0.899 ± 0.01	0.728 ± 0.033	0.864 ± 0.025	0.908 ± 0.01
Semeion	0.819 ± 0.029	0.656 ± 0.077	0.763 ± 0.043	0.885 ± 0.023	0.844 ± 0.019	0.855 ± 0.027	0.869 ± 0.018
Vehicle	0.937 ± 0.017	0.792 ± 0.069	0.885 ± 0.034	0.93 ± 0.012	0.943 ± 0.015	0.899 ± 0.019	0.915 ± 0.029
CIFAR10	0.893 ± 0.0	0.799 ± 0.003	0.856 ± 0.006	0.768 ± 0.009	0.89 ± 0.001	0.882 ± 0.004	0.817 ± 0.004
MNIST	0.858 ± 0.0	0.77 ± 0.008	0.819 ± 0.004	0.754 ± 0.005	0.839 ± 0.002	0.848 ± 0.004	0.739 ± 0.013
USPS	0.877 ± 0.0	0.821 ± 0.006	0.846 ± 0.007	0.764 ± 0.006	0.86 ± 0.005	0.859 ± 0.003	0.754 ± 0.014
Fashion	0.948 ± 0.0	0.869 ± 0.005	0.923 ± 0.002	0.909 ± 0.004	0.941 ± 0.001	0.932 ± 0.003	0.9 ± 0.006
Avg. rank	0.0	1.6	3.1	3.7	4.5	4.65	3.45

Appendix A.2. Results for labeling strategy S2

Table A.5: Balanced accuracy for datasets, for labelling strategy S2 and $c = 0.3$.

Dataset	ORACLE	NAIVE	SAR-EM	LBE	PGLIN	TM	JERM
Breast-w	0.952 ± 0.017	0.597 ± 0.034	0.639 ± 0.03	0.837 ± 0.051	0.717 ± 0.025	0.728 ± 0.042	0.822 ± 0.045
Diabetes	0.716 ± 0.026	0.505 ± 0.006	0.552 ± 0.017	0.706 ± 0.044	0.692 ± 0.031	0.684 ± 0.046	0.723 ± 0.031
Spambase	0.893 ± 0.01	0.636 ± 0.015	0.648 ± 0.021	0.785 ± 0.022	0.677 ± 0.014	0.667 ± 0.015	0.784 ± 0.034
Wdbc	0.971 ± 0.01	0.653 ± 0.033	0.674 ± 0.031	0.705 ± 0.044	0.704 ± 0.043	0.68 ± 0.034	0.764 ± 0.031
Banknote	0.991 ± 0.005	0.633 ± 0.023	0.688 ± 0.023	0.895 ± 0.055	0.726 ± 0.02	0.718 ± 0.032	0.977 ± 0.007
Heart	0.808 ± 0.038	0.562 ± 0.039	0.623 ± 0.025	0.703 ± 0.075	0.726 ± 0.047	0.679 ± 0.058	0.682 ± 0.052
Ionosphere	0.82 ± 0.022	0.507 ± 0.013	0.545 ± 0.036	0.739 ± 0.034	0.767 ± 0.05	0.711 ± 0.052	0.717 ± 0.059
Sonar	0.782 ± 0.049	0.502 ± 0.007	0.568 ± 0.042	0.673 ± 0.074	0.683 ± 0.073	0.583 ± 0.044	0.64 ± 0.041
Haberman	0.511 ± 0.019	0.5 ± 0.0	0.507 ± 0.017	0.58 ± 0.06	0.497 ± 0.039	0.499 ± 0.019	0.575 ± 0.038
Segment	0.985 ± 0.006	0.556 ± 0.015	0.65 ± 0.037	0.93 ± 0.04	0.774 ± 0.037	0.855 ± 0.035	0.933 ± 0.022
Waveform	0.839 ± 0.014	0.566 ± 0.009	0.631 ± 0.031	0.826 ± 0.017	0.666 ± 0.016	0.771 ± 0.016	0.85 ± 0.014
Yeast	0.518 ± 0.01	0.5 ± 0.0	0.504 ± 0.004	0.65 ± 0.016	0.632 ± 0.043	0.61 ± 0.019	0.69 ± 0.017
Musk	0.764 ± 0.014	0.564 ± 0.015	0.61 ± 0.024	0.827 ± 0.022	0.651 ± 0.022	0.743 ± 0.024	0.797 ± 0.014
Isolet	0.603 ± 0.023	0.511 ± 0.006	0.542 ± 0.01	0.862 ± 0.023	0.588 ± 0.027	0.775 ± 0.039	0.814 ± 0.039
Semeion	0.787 ± 0.041	0.548 ± 0.068	0.673 ± 0.03	0.765 ± 0.023	0.748 ± 0.033	0.747 ± 0.036	0.796 ± 0.036
Vehicle	0.937 ± 0.017	0.576 ± 0.032	0.639 ± 0.058	0.835 ± 0.036	0.707 ± 0.042	0.733 ± 0.046	0.85 ± 0.052
CIFAR10	0.893 ± 0.0	0.633 ± 0.002	0.686 ± 0.013	0.833 ± 0.011	0.708 ± 0.004	0.757 ± 0.01	0.855 ± 0.014
MNIST	0.853 ± 0.0	0.609 ± 0.007	0.671 ± 0.016	0.813 ± 0.007	0.7 ± 0.004	0.732 ± 0.008	0.794 ± 0.015
USPS	0.879 ± 0.0	0.622 ± 0.001	0.679 ± 0.009	0.843 ± 0.006	0.706 ± 0.007	0.709 ± 0.004	0.804 ± 0.015
Fashion	0.948 ± 0.0	0.621 ± 0.003	0.683 ± 0.012	0.846 ± 0.011	0.711 ± 0.004	0.722 ± 0.009	0.866 ± 0.008
Avg. rank	0.0	1.1	2.1	5.35	3.65	3.45	5.35

Table A.6: Balanced accuracy for datasets, for labelling strategy S2 and $c = 0.5$.

Dataset	ORACLE	NAIVE	SAR-EM	LBE	PGLIN	TM	JERM
Breast-w	0.952 ± 0.017	0.722 ± 0.035	0.772 ± 0.038	0.886 ± 0.034	0.849 ± 0.035	0.781 ± 0.031	0.902 ± 0.028
Diabetes	0.716 ± 0.026	0.56 ± 0.02	0.626 ± 0.028	0.662 ± 0.038	0.722 ± 0.031	0.685 ± 0.035	0.707 ± 0.045
Spambase	0.893 ± 0.01	0.726 ± 0.016	0.748 ± 0.013	0.871 ± 0.009	0.771 ± 0.015	0.748 ± 0.017	0.84 ± 0.07
Wdbc	0.971 ± 0.01	0.751 ± 0.054	0.783 ± 0.033	0.789 ± 0.036	0.805 ± 0.038	0.76 ± 0.037	0.85 ± 0.04
Banknote	0.991 ± 0.005	0.753 ± 0.024	0.789 ± 0.026	0.929 ± 0.039	0.831 ± 0.021	0.782 ± 0.022	0.99 ± 0.007
Heart	0.808 ± 0.038	0.683 ± 0.04	0.696 ± 0.045	0.731 ± 0.037	0.777 ± 0.025	0.728 ± 0.043	0.707 ± 0.038
Ionosphere	0.82 ± 0.022	0.62 ± 0.063	0.704 ± 0.053	0.748 ± 0.062	0.82 ± 0.043	0.773 ± 0.049	0.757 ± 0.043
Sonar	0.782 ± 0.049	0.56 ± 0.033	0.65 ± 0.065	0.705 ± 0.053	0.726 ± 0.06	0.652 ± 0.064	0.614 ± 0.061
Haberman	0.511 ± 0.019	0.5 ± 0.0	0.509 ± 0.012	0.536 ± 0.032	0.528 ± 0.048	0.519 ± 0.033	0.569 ± 0.046
Segment	0.985 ± 0.006	0.714 ± 0.031	0.808 ± 0.043	0.942 ± 0.025	0.921 ± 0.024	0.915 ± 0.031	0.968 ± 0.012
Waveform	0.839 ± 0.014	0.65 ± 0.012	0.717 ± 0.021	0.845 ± 0.014	0.764 ± 0.02	0.782 ± 0.016	0.85 ± 0.012
Yeast	0.518 ± 0.01	0.501 ± 0.002	0.516 ± 0.007	0.619 ± 0.017	0.654 ± 0.024	0.625 ± 0.012	0.675 ± 0.014
Musk	0.764 ± 0.014	0.648 ± 0.018	0.684 ± 0.022	0.845 ± 0.018	0.754 ± 0.018	0.774 ± 0.022	0.852 ± 0.016
Isolet	0.603 ± 0.023	0.542 ± 0.016	0.587 ± 0.021	0.892 ± 0.015	0.652 ± 0.028	0.807 ± 0.035	0.871 ± 0.026
Semeion	0.787 ± 0.041	0.69 ± 0.033	0.734 ± 0.047	0.806 ± 0.024	0.778 ± 0.04	0.793 ± 0.026	0.817 ± 0.035
Vehicle	0.937 ± 0.017	0.677 ± 0.042	0.778 ± 0.052	0.863 ± 0.028	0.834 ± 0.063	0.777 ± 0.04	0.919 ± 0.038
CIFAR10	0.893 ± 0.0	0.735 ± 0.003	0.778 ± 0.015	0.858 ± 0.007	0.807 ± 0.005	0.786 ± 0.01	0.886 ± 0.007
MNIST	0.853 ± 0.0	0.699 ± 0.003	0.733 ± 0.005	0.816 ± 0.009	0.796 ± 0.002	0.758 ± 0.006	0.788 ± 0.018
USPS	0.879 ± 0.0	0.72 ± 0.005	0.761 ± 0.011	0.85 ± 0.009	0.8 ± 0.003	0.743 ± 0.003	0.825 ± 0.016
Fashion	0.948 ± 0.0	0.747 ± 0.003	0.768 ± 0.007	0.895 ± 0.008	0.824 ± 0.006	0.779 ± 0.007	0.908 ± 0.005
Avg. rank	0.0	1.0	2.25	4.85	4.35	3.3	5.25

Table A.7: Balanced accuracy for datasets, for labelling strategy S2 and $c = 0.7$.

Dataset	ORACLE	NAIVE	SAR-EM	LBE	PGLIN	TM	JERM
Breast-w	0.952 ± 0.017	0.843 ± 0.032	0.87 ± 0.02	0.921 ± 0.027	0.912 ± 0.019	0.86 ± 0.027	0.923 ± 0.019
Diabetes	0.716 ± 0.026	0.626 ± 0.018	0.701 ± 0.033	0.647 ± 0.026	0.756 ± 0.018	0.703 ± 0.033	0.685 ± 0.036
Spambase	0.893 ± 0.01	0.808 ± 0.018	0.829 ± 0.015	0.887 ± 0.016	0.867 ± 0.014	0.83 ± 0.014	0.881 ± 0.011
Wdbc	0.971 ± 0.01	0.86 ± 0.03	0.878 ± 0.032	0.88 ± 0.035	0.912 ± 0.028	0.847 ± 0.035	0.899 ± 0.039
Banknote	0.991 ± 0.005	0.879 ± 0.023	0.91 ± 0.027	0.965 ± 0.021	0.93 ± 0.022	0.882 ± 0.026	0.981 ± 0.006
Heart	0.808 ± 0.038	0.764 ± 0.039	0.786 ± 0.036	0.754 ± 0.032	0.805 ± 0.04	0.767 ± 0.031	0.743 ± 0.061
Ionosphere	0.82 ± 0.022	0.798 ± 0.03	0.805 ± 0.029	0.754 ± 0.029	0.827 ± 0.018	0.814 ± 0.038	0.783 ± 0.049
Sonar	0.782 ± 0.049	0.644 ± 0.04	0.705 ± 0.038	0.733 ± 0.061	0.688 ± 0.05	0.728 ± 0.081	0.659 ± 0.067
Haberman	0.511 ± 0.019	0.505 ± 0.012	0.526 ± 0.028	0.523 ± 0.036	0.528 ± 0.051	0.513 ± 0.022	0.585 ± 0.029
Segment	0.985 ± 0.006	0.881 ± 0.033	0.907 ± 0.025	0.967 ± 0.013	0.969 ± 0.01	0.952 ± 0.016	0.98 ± 0.007
Waveform	0.839 ± 0.014	0.732 ± 0.013	0.781 ± 0.015	0.849 ± 0.007	0.831 ± 0.019	0.806 ± 0.012	0.839 ± 0.009
Yeast	0.518 ± 0.01	0.506 ± 0.006	0.545 ± 0.018	0.617 ± 0.015	0.658 ± 0.029	0.63 ± 0.019	0.652 ± 0.011
Musk	0.764 ± 0.014	0.722 ± 0.015	0.754 ± 0.017	0.836 ± 0.009	0.796 ± 0.014	0.789 ± 0.016	0.863 ± 0.01
Isolet	0.603 ± 0.023	0.566 ± 0.023	0.628 ± 0.028	0.905 ± 0.013	0.715 ± 0.034	0.821 ± 0.029	0.889 ± 0.022
Semeion	0.787 ± 0.041	0.733 ± 0.037	0.783 ± 0.035	0.837 ± 0.037	0.82 ± 0.03	0.809 ± 0.033	0.849 ± 0.034
Vehicle	0.937 ± 0.017	0.811 ± 0.043	0.875 ± 0.039	0.933 ± 0.03	0.916 ± 0.022	0.87 ± 0.042	0.911 ± 0.036
CIFAR10	0.893 ± 0.0	0.828 ± 0.003	0.853 ± 0.005	0.871 ± 0.005	0.874 ± 0.002	0.845 ± 0.002	0.885 ± 0.003
MNIST	0.853 ± 0.0	0.783 ± 0.002	0.814 ± 0.004	0.807 ± 0.007	0.843 ± 0.003	0.809 ± 0.002	0.753 ± 0.033
USPS	0.879 ± 0.0	0.812 ± 0.002	0.831 ± 0.009	0.838 ± 0.011	0.861 ± 0.003	0.812 ± 0.003	0.84 ± 0.013
Fashion	0.948 ± 0.0	0.849 ± 0.002	0.87 ± 0.005	0.918 ± 0.002	0.902 ± 0.004	0.854 ± 0.001	0.925 ± 0.01
Avg. rank	0.0	1.3	3.05	4.25	4.8	3.05	4.55

Appendix A.3. Results for labeling strategy S3

Table A.8: Balanced accuracy for datasets, for labelling strategy S3 and $c = 0.3$.

Dataset	ORACLE	NAIVE	SAR-EM	LBE	PGLIN	TM	JERM
Breast-w	0.952 ± 0.017	0.578 ± 0.022	0.645 ± 0.057	0.868 ± 0.04	0.725 ± 0.049	0.769 ± 0.037	0.846 ± 0.044
Diabetes	0.716 ± 0.026	0.504 ± 0.004	0.549 ± 0.028	0.675 ± 0.054	0.705 ± 0.039	0.665 ± 0.041	0.697 ± 0.034
Spambase	0.892 ± 0.01	0.619 ± 0.011	0.645 ± 0.029	0.86 ± 0.019	0.683 ± 0.012	0.709 ± 0.023	0.834 ± 0.064
Wdbc	0.971 ± 0.01	0.656 ± 0.026	0.688 ± 0.03	0.77 ± 0.04	0.722 ± 0.029	0.707 ± 0.027	0.77 ± 0.042
Banknote	0.991 ± 0.005	0.61 ± 0.021	0.707 ± 0.023	0.959 ± 0.024	0.742 ± 0.023	0.815 ± 0.053	0.982 ± 0.011
Heart	0.808 ± 0.038	0.554 ± 0.022	0.616 ± 0.038	0.713 ± 0.036	0.726 ± 0.054	0.69 ± 0.048	0.7 ± 0.088
Ionosphere	0.82 ± 0.022	0.527 ± 0.031	0.547 ± 0.023	0.739 ± 0.041	0.801 ± 0.038	0.717 ± 0.063	0.667 ± 0.061
Sonar	0.782 ± 0.05	0.507 ± 0.012	0.548 ± 0.038	0.66 ± 0.049	0.73 ± 0.067	0.67 ± 0.047	0.601 ± 0.053
Haberman	0.511 ± 0.019	0.5 ± 0.0	0.509 ± 0.017	0.583 ± 0.064	0.535 ± 0.042	0.506 ± 0.033	0.607 ± 0.065
Segment	0.985 ± 0.006	0.544 ± 0.024	0.671 ± 0.049	0.931 ± 0.038	0.78 ± 0.042	0.889 ± 0.025	0.953 ± 0.029
Waveform	0.837 ± 0.016	0.557 ± 0.007	0.668 ± 0.027	0.823 ± 0.009	0.666 ± 0.014	0.788 ± 0.019	0.844 ± 0.032
Yeast	0.518 ± 0.01	0.5 ± 0.0	0.504 ± 0.005	0.646 ± 0.019	0.608 ± 0.046	0.619 ± 0.022	0.672 ± 0.017
Musk	0.753 ± 0.014	0.574 ± 0.012	0.608 ± 0.019	0.839 ± 0.016	0.632 ± 0.02	0.783 ± 0.022	0.828 ± 0.014
Isolet	0.625 ± 0.03	0.506 ± 0.007	0.535 ± 0.02	0.855 ± 0.036	0.622 ± 0.026	0.81 ± 0.039	0.844 ± 0.027
Semeion	0.804 ± 0.031	0.507 ± 0.015	0.594 ± 0.059	0.793 ± 0.055	0.782 ± 0.043	0.805 ± 0.041	0.8 ± 0.049
Vehicle	0.937 ± 0.017	0.572 ± 0.032	0.676 ± 0.056	0.845 ± 0.041	0.696 ± 0.038	0.789 ± 0.036	0.859 ± 0.041
CIFAR10	0.893 ± 0.0	0.604 ± 0.006	0.694 ± 0.023	0.833 ± 0.006	0.709 ± 0.008	0.793 ± 0.013	0.865 ± 0.009
MNIST	0.851 ± 0.0	0.594 ± 0.004	0.649 ± 0.015	0.798 ± 0.009	0.681 ± 0.004	0.745 ± 0.011	0.76 ± 0.018
USPS	0.884 ± 0.0	0.599 ± 0.006	0.668 ± 0.028	0.825 ± 0.01	0.708 ± 0.003	0.738 ± 0.005	0.75 ± 0.024
Fashion	0.945 ± 0.0	0.613 ± 0.004	0.7 ± 0.008	0.884 ± 0.008	0.718 ± 0.008	0.775 ± 0.008	0.892 ± 0.017
Avg. rank	0.0	1.0	2.1	5.15	3.65	3.9	5.2

Table A.9: Balanced accuracy for datasets, for labelling strategy S3 and $c = 0.5$.

Dataset	ORACLE	NAIVE	SAR-EM	LBE	PGLIN	TM	JERM
Breast-w	0.952 ± 0.017	0.719 ± 0.042	0.777 ± 0.036	0.886 ± 0.028	0.846 ± 0.036	0.8 ± 0.04	0.905 ± 0.039
Diabetes	0.716 ± 0.026	0.565 ± 0.014	0.628 ± 0.023	0.655 ± 0.029	0.72 ± 0.037	0.692 ± 0.034	0.706 ± 0.031
Spambase	0.892 ± 0.01	0.718 ± 0.014	0.736 ± 0.018	0.875 ± 0.014	0.777 ± 0.017	0.75 ± 0.013	0.864 ± 0.086
Wdbc	0.971 ± 0.01	0.761 ± 0.033	0.782 ± 0.035	0.838 ± 0.032	0.813 ± 0.041	0.795 ± 0.031	0.846 ± 0.024
Banknote	0.991 ± 0.005	0.753 ± 0.022	0.829 ± 0.049	0.979 ± 0.01	0.862 ± 0.023	0.795 ± 0.025	0.988 ± 0.005
Heart	0.808 ± 0.038	0.677 ± 0.042	0.719 ± 0.056	0.758 ± 0.037	0.784 ± 0.044	0.731 ± 0.062	0.713 ± 0.09
Ionosphere	0.82 ± 0.022	0.624 ± 0.031	0.696 ± 0.059	0.741 ± 0.043	0.824 ± 0.03	0.774 ± 0.03	0.721 ± 0.053
Sonar	0.782 ± 0.05	0.551 ± 0.049	0.641 ± 0.034	0.715 ± 0.044	0.746 ± 0.054	0.665 ± 0.054	0.624 ± 0.064
Haberman	0.511 ± 0.019	0.503 ± 0.009	0.514 ± 0.018	0.547 ± 0.027	0.523 ± 0.03	0.5 ± 0.019	0.551 ± 0.035
Segment	0.985 ± 0.006	0.71 ± 0.02	0.819 ± 0.033	0.955 ± 0.019	0.914 ± 0.027	0.899 ± 0.02	0.97 ± 0.013
Waveform	0.837 ± 0.016	0.65 ± 0.014	0.727 ± 0.019	0.842 ± 0.013	0.763 ± 0.018	0.782 ± 0.018	0.845 ± 0.019
Yeast	0.518 ± 0.01	0.5 ± 0.001	0.516 ± 0.007	0.621 ± 0.015	0.662 ± 0.024	0.624 ± 0.018	0.66 ± 0.019
Musk	0.753 ± 0.014	0.63 ± 0.017	0.672 ± 0.029	0.847 ± 0.014	0.741 ± 0.02	0.78 ± 0.017	0.837 ± 0.019
Isolet	0.625 ± 0.03	0.532 ± 0.01	0.593 ± 0.019	0.896 ± 0.02	0.685 ± 0.025	0.843 ± 0.033	0.88 ± 0.022
Semeion	0.804 ± 0.031	0.649 ± 0.044	0.712 ± 0.065	0.807 ± 0.035	0.798 ± 0.028	0.81 ± 0.03	0.829 ± 0.036
Vehicle	0.937 ± 0.017	0.675 ± 0.027	0.76 ± 0.038	0.875 ± 0.034	0.839 ± 0.052	0.776 ± 0.053	0.88 ± 0.053
CIFAR10	0.893 ± 0.0	0.738 ± 0.009	0.782 ± 0.015	0.845 ± 0.003	0.824 ± 0.004	0.797 ± 0.008	0.883 ± 0.005
MNIST	0.851 ± 0.0	0.694 ± 0.003	0.738 ± 0.015	0.801 ± 0.009	0.797 ± 0.002	0.754 ± 0.004	0.791 ± 0.024
USPS	0.884 ± 0.0	0.717 ± 0.004	0.745 ± 0.019	0.829 ± 0.008	0.811 ± 0.004	0.748 ± 0.004	0.786 ± 0.022
Fashion	0.945 ± 0.0	0.741 ± 0.004	0.764 ± 0.012	0.889 ± 0.007	0.836 ± 0.004	0.777 ± 0.004	0.916 ± 0.007
Avg. rank	0.0	1.05	2.2	4.95	4.4	3.4	5.0

Table A.10: Balanced accuracy for datasets, for labelling strategy S3 and $c = 0.7$.

Dataset	ORACLE	NAIVE	SAR-EM	LBE	PGLIN	TM	JERM
Breast-w	0.952 ± 0.017	0.844 ± 0.024	0.887 ± 0.016	0.912 ± 0.029	0.919 ± 0.023	0.876 ± 0.028	0.942 ± 0.019
Diabetes	0.716 ± 0.026	0.62 ± 0.026	0.696 ± 0.032	0.656 ± 0.018	0.754 ± 0.02	0.708 ± 0.033	0.692 ± 0.024
Spambase	0.892 ± 0.01	0.794 ± 0.015	0.818 ± 0.015	0.844 ± 0.115	0.872 ± 0.013	0.841 ± 0.016	0.842 ± 0.095
Wdbc	0.971 ± 0.01	0.86 ± 0.028	0.875 ± 0.026	0.909 ± 0.037	0.906 ± 0.029	0.867 ± 0.021	0.875 ± 0.043
Banknote	0.991 ± 0.005	0.887 ± 0.03	0.906 ± 0.023	0.971 ± 0.02	0.954 ± 0.013	0.896 ± 0.021	0.982 ± 0.005
Heart	0.808 ± 0.038	0.771 ± 0.035	0.789 ± 0.042	0.749 ± 0.056	0.805 ± 0.05	0.778 ± 0.031	0.768 ± 0.079
Ionosphere	0.82 ± 0.022	0.802 ± 0.027	0.791 ± 0.036	0.748 ± 0.037	0.821 ± 0.02	0.826 ± 0.035	0.776 ± 0.032
Sonar	0.782 ± 0.05	0.648 ± 0.073	0.711 ± 0.055	0.743 ± 0.056	0.681 ± 0.057	0.712 ± 0.047	0.682 ± 0.065
Haberman	0.511 ± 0.019	0.507 ± 0.013	0.527 ± 0.027	0.537 ± 0.041	0.527 ± 0.038	0.506 ± 0.031	0.542 ± 0.039
Segment	0.985 ± 0.006	0.886 ± 0.048	0.916 ± 0.026	0.965 ± 0.019	0.972 ± 0.009	0.947 ± 0.02	0.978 ± 0.008
Waveform	0.837 ± 0.016	0.729 ± 0.019	0.782 ± 0.02	0.852 ± 0.008	0.839 ± 0.015	0.818 ± 0.021	0.824 ± 0.016
Yeast	0.518 ± 0.01	0.505 ± 0.005	0.544 ± 0.016	0.629 ± 0.015	0.644 ± 0.032	0.637 ± 0.013	0.656 ± 0.011
Musk	0.753 ± 0.014	0.691 ± 0.023	0.725 ± 0.023	0.842 ± 0.011	0.787 ± 0.016	0.789 ± 0.018	0.856 ± 0.01
Isolet	0.625 ± 0.03	0.576 ± 0.021	0.641 ± 0.029	0.909 ± 0.015	0.733 ± 0.018	0.834 ± 0.024	0.899 ± 0.011
Semeion	0.804 ± 0.031	0.772 ± 0.046	0.797 ± 0.039	0.859 ± 0.035	0.82 ± 0.025	0.817 ± 0.027	0.873 ± 0.024
Vehicle	0.937 ± 0.017	0.798 ± 0.044	0.881 ± 0.031	0.934 ± 0.017	0.925 ± 0.023	0.853 ± 0.044	0.902 ± 0.031
CIFAR10	0.893 ± 0.0	0.825 ± 0.003	0.846 ± 0.005	0.855 ± 0.015	0.882 ± 0.001	0.853 ± 0.005	0.873 ± 0.006
MNIST	0.851 ± 0.0	0.79 ± 0.002	0.81 ± 0.005	0.796 ± 0.011	0.846 ± 0.002	0.813 ± 0.002	0.797 ± 0.024
USPS	0.884 ± 0.0	0.812 ± 0.005	0.83 ± 0.007	0.834 ± 0.008	0.864 ± 0.002	0.826 ± 0.005	0.816 ± 0.016
Fashion	0.945 ± 0.0	0.849 ± 0.003	0.869 ± 0.008	0.916 ± 0.004	0.913 ± 0.002	0.868 ± 0.002	0.929 ± 0.012
Avg. rank	0.0	1.3	2.9	4.3	4.75	3.3	4.45

Appendix A.4. Results for labeling strategy S4

Table A.11: balanced accuracy for datasets, for labelling strategy S4 and $c = 0.3$.

Dataset	ORACLE	NAIVE	SAR-EM	LBE	PGLIN	TM	JERM
Breast-w	0.952 ± 0.017	0.599 ± 0.016	0.638 ± 0.033	0.75 ± 0.038	0.723 ± 0.037	0.659 ± 0.043	0.783 ± 0.031
Diabetes	0.716 ± 0.026	0.511 ± 0.009	0.566 ± 0.009	0.722 ± 0.027	0.683 ± 0.041	0.639 ± 0.029	0.726 ± 0.023
Spambase	0.893 ± 0.01	0.64 ± 0.011	0.645 ± 0.011	0.677 ± 0.06	0.67 ± 0.013	0.658 ± 0.014	0.763 ± 0.029
Wdbc	0.971 ± 0.01	0.648 ± 0.032	0.667 ± 0.04	0.678 ± 0.044	0.692 ± 0.039	0.67 ± 0.034	0.749 ± 0.038
Banknote	0.991 ± 0.005	0.64 ± 0.017	0.665 ± 0.024	0.767 ± 0.025	0.713 ± 0.02	0.676 ± 0.02	0.961 ± 0.017
Heart	0.808 ± 0.038	0.599 ± 0.037	0.613 ± 0.033	0.705 ± 0.058	0.721 ± 0.056	0.651 ± 0.05	0.679 ± 0.031
Ionosphere	0.82 ± 0.022	0.523 ± 0.029	0.547 ± 0.036	0.756 ± 0.052	0.743 ± 0.069	0.657 ± 0.058	0.697 ± 0.071
Sonar	0.782 ± 0.049	0.524 ± 0.031	0.56 ± 0.035	0.675 ± 0.057	0.716 ± 0.07	0.595 ± 0.074	0.597 ± 0.057
Haberman	0.511 ± 0.019	0.5 ± 0.0	0.512 ± 0.018	0.569 ± 0.072	0.534 ± 0.057	0.505 ± 0.023	0.615 ± 0.068
Segment	0.985 ± 0.006	0.579 ± 0.023	0.646 ± 0.033	0.842 ± 0.025	0.758 ± 0.039	0.812 ± 0.034	0.88 ± 0.029
Waveform	0.84 ± 0.015	0.582 ± 0.012	0.623 ± 0.015	0.776 ± 0.018	0.651 ± 0.014	0.719 ± 0.023	0.822 ± 0.035
Yeast	0.518 ± 0.01	0.5 ± 0.0	0.507 ± 0.006	0.662 ± 0.014	0.66 ± 0.041	0.628 ± 0.011	0.693 ± 0.022
Musk	0.754 ± 0.014	0.585 ± 0.012	0.628 ± 0.018	0.778 ± 0.02	0.652 ± 0.022	0.689 ± 0.021	0.742 ± 0.02
Isolet	0.602 ± 0.026	0.525 ± 0.008	0.553 ± 0.022	0.803 ± 0.051	0.6 ± 0.027	0.741 ± 0.029	0.756 ± 0.032
Semeion	0.786 ± 0.027	0.605 ± 0.067	0.667 ± 0.063	0.726 ± 0.037	0.751 ± 0.031	0.722 ± 0.041	0.77 ± 0.044
Vehicle	0.937 ± 0.017	0.598 ± 0.037	0.626 ± 0.03	0.753 ± 0.049	0.699 ± 0.033	0.666 ± 0.062	0.799 ± 0.061
CIFAR10	0.895 ± 0.0	0.645 ± 0.003	0.674 ± 0.004	0.783 ± 0.01	0.701 ± 0.003	0.708 ± 0.005	0.786 ± 0.01
MNIST	0.848 ± 0.0	0.621 ± 0.004	0.648 ± 0.004	0.778 ± 0.008	0.677 ± 0.006	0.667 ± 0.004	0.77 ± 0.008
USPS	0.882 ± 0.0	0.624 ± 0.004	0.66 ± 0.003	0.769 ± 0.003	0.692 ± 0.004	0.676 ± 0.003	0.78 ± 0.006
Fashion	0.949 ± 0.0	0.641 ± 0.003	0.666 ± 0.006	0.779 ± 0.006	0.708 ± 0.002	0.688 ± 0.003	0.805 ± 0.007
Avg. rank	0.0	1.0	2.05	5.1	4.1	3.2	5.55

Table A.12: balanced accuracy for datasets, for labelling strategy S4 and $c = 0.5$.

Dataset	ORACLE	NAIVE	SAR-EM	LBE	PGLIN	TM	JERM
Breast-w	0.952 ± 0.017	0.733 ± 0.029	0.758 ± 0.036	0.848 ± 0.029	0.828 ± 0.028	0.766 ± 0.033	0.859 ± 0.019
Diabetes	0.716 ± 0.026	0.579 ± 0.017	0.637 ± 0.03	0.679 ± 0.039	0.722 ± 0.031	0.689 ± 0.034	0.714 ± 0.031
Spambase	0.893 ± 0.01	0.732 ± 0.014	0.743 ± 0.013	0.816 ± 0.016	0.77 ± 0.015	0.746 ± 0.015	0.799 ± 0.078
Wdbc	0.971 ± 0.01	0.76 ± 0.04	0.787 ± 0.046	0.806 ± 0.039	0.791 ± 0.043	0.762 ± 0.043	0.852 ± 0.028
Banknote	0.991 ± 0.005	0.75 ± 0.023	0.784 ± 0.021	0.86 ± 0.031	0.815 ± 0.019	0.768 ± 0.021	0.986 ± 0.008
Heart	0.808 ± 0.038	0.7 ± 0.042	0.712 ± 0.048	0.76 ± 0.049	0.776 ± 0.028	0.707 ± 0.061	0.727 ± 0.034
Ionosphere	0.82 ± 0.022	0.625 ± 0.047	0.663 ± 0.057	0.769 ± 0.056	0.829 ± 0.024	0.755 ± 0.037	0.738 ± 0.033
Sonar	0.782 ± 0.049	0.581 ± 0.059	0.649 ± 0.057	0.698 ± 0.041	0.738 ± 0.058	0.671 ± 0.059	0.649 ± 0.048
Haberman	0.511 ± 0.019	0.499 ± 0.003	0.509 ± 0.021	0.542 ± 0.027	0.56 ± 0.064	0.515 ± 0.024	0.596 ± 0.061
Segment	0.985 ± 0.006	0.707 ± 0.032	0.781 ± 0.033	0.903 ± 0.035	0.872 ± 0.031	0.88 ± 0.024	0.964 ± 0.014
Waveform	0.84 ± 0.015	0.658 ± 0.014	0.712 ± 0.015	0.835 ± 0.011	0.753 ± 0.013	0.767 ± 0.02	0.854 ± 0.014
Yeast	0.518 ± 0.01	0.5 ± 0.001	0.512 ± 0.008	0.637 ± 0.014	0.672 ± 0.026	0.632 ± 0.018	0.681 ± 0.029
Musk	0.754 ± 0.014	0.664 ± 0.024	0.693 ± 0.023	0.842 ± 0.018	0.746 ± 0.017	0.752 ± 0.02	0.839 ± 0.017
Isolet	0.602 ± 0.026	0.547 ± 0.017	0.578 ± 0.026	0.864 ± 0.024	0.645 ± 0.025	0.8 ± 0.044	0.847 ± 0.03
Semeion	0.786 ± 0.027	0.694 ± 0.033	0.723 ± 0.036	0.785 ± 0.04	0.773 ± 0.03	0.756 ± 0.039	0.832 ± 0.035
Vehicle	0.937 ± 0.017	0.697 ± 0.048	0.75 ± 0.056	0.86 ± 0.052	0.813 ± 0.047	0.764 ± 0.054	0.895 ± 0.034
CIFAR10	0.895 ± 0.0	0.738 ± 0.002	0.771 ± 0.007	0.844 ± 0.005	0.796 ± 0.004	0.776 ± 0.003	0.871 ± 0.004
MNIST	0.848 ± 0.0	0.704 ± 0.004	0.742 ± 0.009	0.827 ± 0.007	0.786 ± 0.003	0.742 ± 0.002	0.822 ± 0.009
USPS	0.882 ± 0.0	0.724 ± 0.005	0.738 ± 0.011	0.833 ± 0.009	0.797 ± 0.003	0.737 ± 0.004	0.84 ± 0.01
Fashion	0.949 ± 0.0	0.749 ± 0.005	0.771 ± 0.007	0.862 ± 0.006	0.809 ± 0.004	0.764 ± 0.002	0.878 ± 0.012
Avg. rank	0.0	1.0	2.25	5.0	4.3	3.1	5.35

Table A.13: balanced accuracy for datasets, for labelling strategy S4 and $c = 0.7$.

Dataset	ORACLE	NAIVE	SAR-EM	LBE	PGLIN	TM	JERM
Breast-w	0.952 ± 0.017	0.852 ± 0.02	0.877 ± 0.022	0.907 ± 0.023	0.906 ± 0.016	0.865 ± 0.028	0.917 ± 0.021
Diabetes	0.716 ± 0.026	0.632 ± 0.027	0.698 ± 0.032	0.653 ± 0.031	0.753 ± 0.026	0.703 ± 0.031	0.691 ± 0.028
Spambase	0.893 ± 0.01	0.811 ± 0.016	0.822 ± 0.014	0.858 ± 0.12	0.864 ± 0.014	0.828 ± 0.017	0.799 ± 0.142
Wdbc	0.971 ± 0.01	0.865 ± 0.035	0.883 ± 0.029	0.886 ± 0.036	0.903 ± 0.025	0.865 ± 0.035	0.904 ± 0.023
Banknote	0.991 ± 0.005	0.871 ± 0.024	0.893 ± 0.023	0.938 ± 0.019	0.924 ± 0.02	0.876 ± 0.025	0.98 ± 0.007
Heart	0.808 ± 0.038	0.75 ± 0.035	0.795 ± 0.038	0.789 ± 0.048	0.817 ± 0.029	0.774 ± 0.035	0.77 ± 0.048
Ionosphere	0.82 ± 0.022	0.784 ± 0.034	0.817 ± 0.031	0.772 ± 0.034	0.826 ± 0.036	0.814 ± 0.046	0.776 ± 0.04
Sonar	0.782 ± 0.049	0.657 ± 0.065	0.739 ± 0.061	0.749 ± 0.052	0.705 ± 0.029	0.706 ± 0.031	0.675 ± 0.092
Haberman	0.511 ± 0.019	0.499 ± 0.003	0.527 ± 0.02	0.536 ± 0.02	0.538 ± 0.063	0.531 ± 0.044	0.55 ± 0.027
Segment	0.985 ± 0.006	0.885 ± 0.021	0.906 ± 0.024	0.947 ± 0.019	0.962 ± 0.016	0.932 ± 0.023	0.98 ± 0.006
Waveform	0.84 ± 0.015	0.735 ± 0.014	0.779 ± 0.014	0.854 ± 0.007	0.828 ± 0.012	0.803 ± 0.015	0.837 ± 0.009
Yeast	0.518 ± 0.01	0.506 ± 0.005	0.549 ± 0.018	0.628 ± 0.015	0.637 ± 0.024	0.637 ± 0.016	0.662 ± 0.018
Musk	0.754 ± 0.014	0.712 ± 0.015	0.746 ± 0.02	0.869 ± 0.01	0.788 ± 0.016	0.785 ± 0.017	0.865 ± 0.01
Isolet	0.602 ± 0.026	0.572 ± 0.018	0.629 ± 0.019	0.899 ± 0.017	0.696 ± 0.033	0.81 ± 0.035	0.882 ± 0.01
Semeion	0.786 ± 0.027	0.74 ± 0.039	0.771 ± 0.039	0.815 ± 0.033	0.801 ± 0.027	0.797 ± 0.031	0.877 ± 0.029
Vehicle	0.937 ± 0.017	0.807 ± 0.043	0.871 ± 0.034	0.917 ± 0.03	0.92 ± 0.025	0.872 ± 0.022	0.91 ± 0.024
CIFAR10	0.895 ± 0.0	0.827 ± 0.001	0.845 ± 0.004	0.881 ± 0.004	0.869 ± 0.002	0.839 ± 0.002	0.881 ± 0.017
MNIST	0.848 ± 0.0	0.792 ± 0.003	0.821 ± 0.003	0.813 ± 0.005	0.84 ± 0.002	0.81 ± 0.002	0.803 ± 0.013
USPS	0.882 ± 0.0	0.817 ± 0.003	0.824 ± 0.002	0.852 ± 0.01	0.856 ± 0.001	0.818 ± 0.005	0.868 ± 0.014
Fashion	0.949 ± 0.0	0.845 ± 0.003	0.856 ± 0.005	0.914 ± 0.004	0.895 ± 0.002	0.85 ± 0.004	0.929 ± 0.004
Avg. rank	0.0	1.15	3.05	4.45	4.75	3.05	4.55

Appendix B.

Lemma 1. Let z_1, \dots, z_n be fixed vectors from \mathcal{Z} . Besides, let \mathcal{F} be a family of K -dimensional functions on \mathcal{Z} . We also consider Lipschitz functions $h_i : \mathbb{R}^K \rightarrow \mathbb{R}, i = 1, \dots, n$ with a Lipschitz constant $L > 0$. If there exists $\bar{f} \in \mathcal{F}$ such that $h_i(\bar{f}(z_i)) = 0$ for $i = 1, \dots, n$, then

$$\mathbb{E} \sup_{f \in \mathcal{F}} \left| \sum_{i=1}^n \varepsilon_i h_i(f(z_i)) \right| \leq 2\sqrt{2}L \mathbb{E} \sup_{f \in \mathcal{F}} \sum_{i=1}^n \sum_{k=1}^K \varepsilon_{i,k} f_k(z_i), \quad (\text{B.1})$$

where $f = (f_1, f_2, \dots, f_K)$ for each $f \in \mathcal{F}$ and $\{\varepsilon_i\}_i, \{\varepsilon_{i,k}\}_{i,k}$ are independent Rademacher sequences.

Proof. The key step in the proof is Corollary 1 in [37], which does not require the assumption on existence of \bar{f} to establish analogue of the lemma above without absolute values on the left-hand side of (B.1). We show how to strengthen Corollary 1 in [37] to (B.1). The price for this improvement will be the additional constant 2 on the right-hand side of the inequality.

For all real t we have $|t| = \max(t, 0) + \max(-t, 0)$. Therefore, we obtain

$$\begin{aligned} \mathbb{E} \sup_{f \in \mathcal{F}} \left| \sum_{i=1}^n \varepsilon_i h_i(f(z_i)) \right| &= \mathbb{E} \sup_{f \in \mathcal{F}} \left[\max \left(\sum_{i=1}^n \varepsilon_i h_i(f(z_i)), 0 \right) + \max \left(-\sum_{i=1}^n \varepsilon_i h_i(f(z_i)), 0 \right) \right] \\ &\leq \mathbb{E} \sup_{f \in \mathcal{F}} \max \left(\sum_{i=1}^n \varepsilon_i h_i(f(z_i)), 0 \right) + \mathbb{E} \sup_{f \in \mathcal{F}} \max \left(\sum_{i=1}^n (-\varepsilon_i) h_i(f(z_i)), 0 \right). \end{aligned} \quad (\text{B.2})$$

Variables ε_i and $-\varepsilon_i$ have the same distribution, so (B.2) equals

$$2\mathbb{E} \sup_{f \in \mathcal{F}} \max \left(\sum_{i=1}^n \varepsilon_i h_i(f(z_i)), 0 \right) = 2\mathbb{E} \max \left(\sup_{f \in \mathcal{F}} \sum_{i=1}^n \varepsilon_i h_i(f(z_i)), 0 \right),$$

which is $2\mathbb{E} \sup_{f \in \mathcal{F}} \sum_{i=1}^n \varepsilon_i h_i(f(z_i))$, because

$$\sup_{f \in \mathcal{F}} \sum_{i=1}^n \varepsilon_i h_i(f(z_i)) \geq \sum_{i=1}^n \varepsilon_i h_i(\bar{f}(z_i)) = 0.$$

Finally, we apply Corollary 1 in [37].

□